Centre for Geo-Information

Thesis Report GIRS-2008-20

Application of continuum removal technique to the water absorption features in the NIR region to estimate canopy water content

Taeibah Abdi

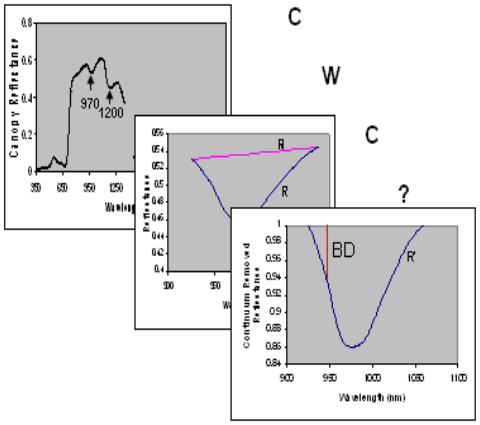

DECEMBER 2008

WAGENINGEN UNIVERSITY
WAGENINGEN UR

Application of the continuum removal technique to the water absorption features in the NIR region to estimate canopy water content

Taeibah Abdi

Registration number 800827-003-080

Supervisors:

dr. ir. J. Clevers

dr. ir. L. Kooistra

A thesis submitted in partial fulfilment of the degree of Master of Science
at Wageningen University and Research Centre,
The Netherlands.

December 2008

Wageningen, the Netherlands

Thesis code number: GRS-80439
Thesis Report: GIRS-2008-20
Wageningen University and Research Centre
Laboratory of Geo-information Science and Remote Sensing

Foreword

This Report is my MSc thesis done as part of the Master of Science in Geo-Information Science (MGI) at the Wageningen University. The report is about application of the continuum removal technique to the water absorption features in NIR.

My deep appreciation goes to my supervisors Dr. Jan Clevers and Dr. Lammert Kooistra for their invaluable encouragements, ideas, suggestions and patience during my research work. Without their advice and support this thesis would never have become feasible.

I would like to extend my special thanks to my husband Hadi and daughter Mozhdeh for their courage and support during the entire period of my thesis work.

Taeibah Abdi, December 2008

Table of content:

List of figures

List of tables:

ABBREVIATIONS:

CWC	Canopy water content
WBI	Water band index
NDWI	Normalized difference water index
NDVI	Normalized difference vegetation index
NDII	Normalized Difference Infrared Index
MSI	Moisture Stress Index
EWT	Equivalent water thickness
FW	Fresh weight
DW	Dry weight
BD	Band depth
Dc	Band center
NBD	Normalized band depth
MBD	Maximum band depth
AUC	Area under continuum
NIR	Near infrared
VALERI	Validation of Land European Remote sensing Instruments
Df	Degrees of freedom

ABSTRACT

Biogeochemical processes in plants, such as photosynthesis, evaporation and net primary production, are directly related to foliar water. Therefore, the canopy water content (CWC) is important for understanding of the terrestrial ecosystem functioning. Spectral information related to the water absorption features at 970 nm and 1200 nm offers possibilities for deriving information on CWC.
The objective of this study was to find which interval around the water absorption features at 970 nm and 1200 nm should be selected to apply the continuum removal technique for estimating CWC and biomass, and which index or indices based on the continuum removal technique are stronger on estimation canopy biophysical variables and finally compare the results of the continuum removal to those based on spectral indices and derivative spectra. The feasibility of using information from the water absorption features in the near-infrared (NIR) region of the spectrum was tested by estimating canopy water content for two test sites with different canopy structure. The first site is a heterogeneous natural area in the floodplain Millingerwaard along the river Waal in the Netherlands. The other site is an extensively managed grasslands which is located as a buffer zone around a central rewetted bog ecosystem in the Achterhoek near Winterswijk. Spectral information at both test sites was obtained with an ASD FieldSpec spectrometer, whereas at the first site HyMap airborne imaging spectrometer data were also acquired.

Based on these datasets the best interval to apply the continuum removal technique at these water absorption features is the broader one which includes the whole absorption feature at 970 and 1200 nm.
Results yielded that maximum band depth (MBD) and area under the curve (AUC) have clearly stronger correlation with biophysical variables than other continuum removal indicators at both water absorption features in the NIR region in a homogeneous area, while MBD/AUC and AUC/MBD at 970 nm have higher correlation with canopy biophysical variables in a heterogeneous area.
Result also showed that the first derivative of spectra is better than indices derived from the continuum removal and WBI and NDWI on estimation of canopy biophysical variables in a heterogeneous area and MBD and AUC based on the continuum removal technique in a homogeneous area yielded a stronger effect on estimation of canopy biophysical variables.

Key words: Canopy water content, fresh weight, dry weight, Field spectrometer, Continuum removal technique, Derivative spectra, Spectral indices, Remote sensing

1 INTRODUCTION

1.1 Background

Currently one of the main scientific issues is to understand and quantify the impact of global climate change on the Earth system. One of the challenges of the coming decades is the understanding of the role of terrestrial ecosystems and the changes they may undergo. The water cycle is one of its most important characteristics (ESA, 2006). In this respect, the canopy water content is of interest in many applications. Estimates of vegetation water content are of interest for assessing vegetation water status in agriculture and forestry (Gao, 1996; Gao & Goetz, 1995; Penuelas et al., 1997; Ustin et al., 2004a,b, 1998; Zarco-Tejada et al., 2003), and have been used for drought assessment (Penuelas et al., 1993) and prediction of susceptibility to wildfire (Chuvieco et al., 2004; Riano et al., 2005; Ustin et al., 1998). Thus, canopy water content is important for the understanding of the functioning of the terrestrial ecosystem (Running & Coughlan, 1988).

Water absorption features as a result of absorption by O-H bonds in water can be found at approximately 970, 1200, 1450 and 1950 nm (Curran, 1989). The features at 1450 and 1950 nm are most pronounced. However, in those spectral bands atmospheric absorption by water vapor is that strong that hardly any radiation is reaching the Earth surface. As a result, those bands will result in very noisy measurements and should not be used for remote sensing. The features at 970 and 1200 nm are not that pronounced, but still clearly observable (Danson et al., 1992; Sims & Gamon, 2003). Therefore, these offer interesting possibilities for deriving information on leaf and canopy water content. However, in these regions also minor absorption features due to atmospheric water vapor occur at 940 and 1140 nm (lqbal, 1983). These are shifted somewhat to shorter wavelengths in comparison to the liquid water bands caused by water in the canopy. Figure 1 illustrates water absorption features in the infrared region for some spectral measurements on natural vegetation plots. The position of the liquid water absorption features at 970 nm and 1200 nm are indicated.

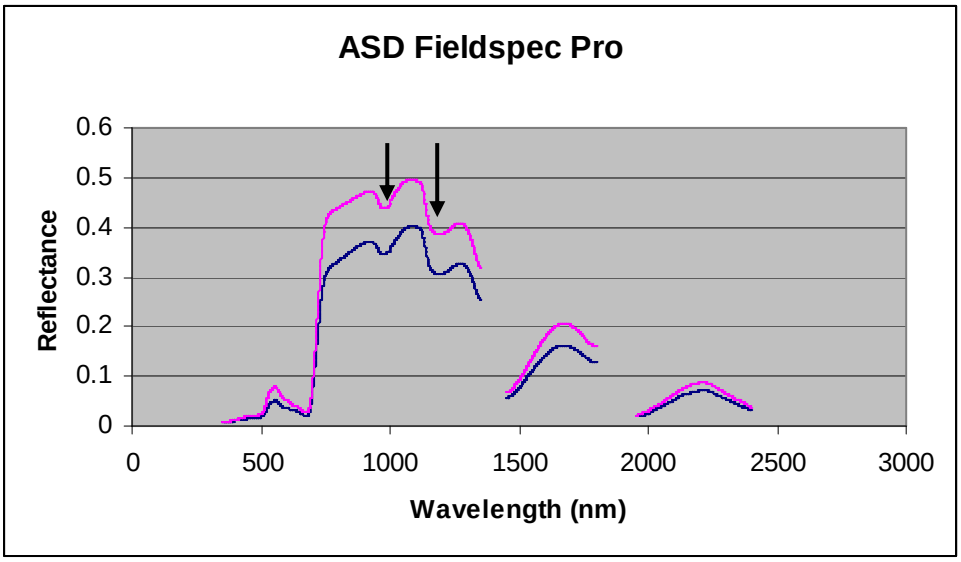

Figure 1: Example of two spectral signatures of Millingerwaard plots measured with the ASD FieldSpec Pro.

1.2 Problem definition

For quantifying the water content, at the canopy level the canopy water content (CWC) can be defined as the quantity of water per unit area of ground surface and thus can be given in g m^{-2} (Ceccato et al., 2002) or in kgm^{-2} by converting EWT to the appropriate units:

$$CWC = LAI \times EWT \quad (1)$$

Where EWT is the equivalent water thickness and defined as the quantity of water per unit leaf area in g cm^{-2} (Danson et al., 1992).

Another way of calculating CWC is by taking the difference between fresh weight (FW in kg m^{-2}) and dry weight (DW in kg m^{-2}):

$$CWC = FW - DW \quad (2)$$

Various approaches have been developed for estimation of water content in plants. These can be divided broadly into spectral indices and techniques based on the inversion of radiative transfer models. Water content sensitive spectral indices are typically combinations between reflectance at wavelengths where water absorbs energy at different magnitudes. Spectral indices that have been developed using these water bands are: Water Band Index (WBI), Water Band Index normalized with NDVI (WBI/NDVI), and Normalized Difference Water Index (NDWI). Also the first derivative of the spectral signature has been used in the NIR region. Most of these indices are similar to those which have been applied in the red-edge spectral region to estimate chlorophyll content such as Simple Ratio and the Normalized Difference Vegetation Index (Rouse et al., 1973; Tucker 1979; Sellers 1985). Continuum removal techniques also have been applied in the red-edge spectral region. However, there have been surprisingly few studies that have applied this technique to the water absorption features in the NIR region and examined the relationships between canopy water content and indicators derived from the continuum removal technique.

1.3 Research objective

The aim of this thesis is to apply the continuum removal technique to the water absorption features in the NIR region to estimate canopy water content and biomass. Aim is also to compare the results of the continuum removal to those based on other approaches such as WBI, NDWI and first derivative spectra.

1.4 Research questions

1) Which spectral interval should be used to apply the continuum removal technique to the water absorption features at 970 nm and 1200 nm?

2) Which index based on the continuum removal technique (maximum band depth, area under the curve or MBD/ Area) is best for estimating canopy water content?

3) Are these results more accurate than WBI, NDWI, and first derivative of spectra?

1.5 Report outline

The general background information of the research was introduced in chapter one. This includes the problem definition, research objectives, research questions, and report outline. Chapter two reviews available methods for CWC estimation. Chapter three includes study area and data which have been available. The implementation of the continuum removal technique and previous methods is discussed in Chapter four. Chapter five presents the results of the application of the new method, continuum removal, and other methods on the Millingerwaard and Achterhoek areas. Chapter five discusses the results with regard to the research questions. Finally, chapter 6 lists the conclusions and recommendations raised from the study. The appendices are given at the end of the report.

2 LITERATURE REVIEW

2.1 Overview – CWC estimation

Because water has several absorption maxima throughout the infrared region of the spectrum (Palmer & Williams, 1974), quite a number of different spectral indices based on a ratio, or some other simple mathematical formula of reflectance at two or more wavelengths (Ceccato et al., 2002; Gao & Goetz, 1995; Gao, 1996; Penuelas et al., 1993; Serrano et al., 2000; Ustin et al., 1998).), first derivative of spectral reflectance (Clevers & Kooistra, 2006), and continuum removal techniques (Tian et al., 2001) have been developed for estimation of water content.

2.2 Spectral indices

2.3.1 Water Band Index

The simplest water index is a ratio between reflectance at a reference wavelength where water does not absorb and a wavelength where water does absorb. One example of this is the water band index (WBI). The Water Band Index is a reflectance measurement that is sensitive to changes in canopy water status. As the water content of vegetation canopies increases, the strength of the absorption around 970 nm increases relative to that of 900 nm (Penuelas et al. 1993; Champagne et al. 2001). WBI is defined by the following equation:

$$WBI = \frac{\rho 900}{\rho 970} \qquad (3)$$

Where $\rho\,900$ and $\rho\,970$ are the spectral reflectance at 900 and 970 nm, respectively. The common rang for green vegetation is 0.8 to 1.2.

Sims and Gamon (2003) generalized WBIxxx, which is defined by the equation (4). This water band index tests the effect of variation in the strength of light absorption by water across the spectrum:

$$WBIxxx = \frac{\rho 900}{\rho xxx} \qquad (4)$$

Where the reference wavelength is held constant at 900 nm but the index wavelength (xxx) is varied.

2.3.3 Normalized Difference Water Index

The Normalized Difference Water Index (NDWI) is sensitive to changes in vegetation canopy water content because reflectance at 860 nm and 1240 nm has similar but slightly different liquid water absorption properties. The scattering of light by vegetation canopies enhances the weak liquid water absorption at 1240 nm. Applications include forest canopy stress analysis, leaf area index studies in densely foliated vegetation, plant productivity modeling, and fire susceptibility studies (Gao, 1996). NDWI is defined by the following equation:

$$NDWI = \frac{\rho 860 - \rho 1240}{\rho 860 + \rho 1240} \qquad (5)$$

Where $\rho 860$ and $\rho 1240$ are the spectral reflectance at 860 and 1240 nm, respectively. The value of this index ranges from -1 to 1. The common range for green vegetation is -0.1 to 0.4.

2.3.4 Moisture Stress Index

The Moisture Stress Index (MSI) is a reflectance measurement that is sensitive to increasing leaf water content. As the water content of leaves in vegetation canopies increases, the strength of the absorption around 1599 nm increases. Absorption at 819 nm is nearly unaffected by changing water content, so it is used as the reference. Applications include canopy stress analysis, productivity prediction and modeling, fire hazard condition analysis, and studies of ecosystem physiology. The MSI is inverted relative to the other water VIs; higher values indicate greater water stress and less water content (Hunt et al. 1989; Ceccato et al. 2002). MSI is defined by the following equation:

$$MSI = \frac{\rho 1599}{\rho 819} \qquad (6)$$

The value of this index ranges from 0 to more than 3. The common range for green vegetation is 0.4 to 2.

2.3.5 Normalized Difference Infrared Index

The Normalized Difference Infrared Index (NDII) is a reflectance measurement that is sensitive to changes in water content of plant canopies. The NDII uses a normalized difference formulation instead of a simple ratio, and the index values increase with increasing water content. Applications include crop agricultural management, forest canopy monitoring, and vegetation stress detection (Hardisky et al., 1983; Jackson et al. 2004). NDII is defined by the following equation:

$$\text{NDII} = \frac{\rho 819 - \rho 1649}{\rho 819 + \rho 1649} \qquad (7)$$

The value of this index ranges from -1 to 1. The common range for green vegetation is 0.02 to 0.6.

2.4 First derivative of spectra

First derivative of the reflectance spectrum corresponds to the slopes of the absorption features. It's defined by the following equation:

$$\text{First derivative of spectra at } (\lambda + 0.5) = \frac{\rho_{\lambda+1} - \rho_{\lambda}}{\lambda + 1 - \lambda} \qquad (8)$$

Where λ refers to channels in the absorption feature.
It provides better correlation with leaf water content than those obtained from the direct correlation with reflectance (Clevers & Kooistra, 2006).

2.5 Continuum removal

The continuum is an estimate of the other absorptions present in the spectrum, not including the one of interest (figure 2a). Once the continuum line is established, continuum-removed spectra for the absorption features are calculated by dividing the original reflectance spectrum by the corresponding reflectance of the continuum line (Figure 2b).

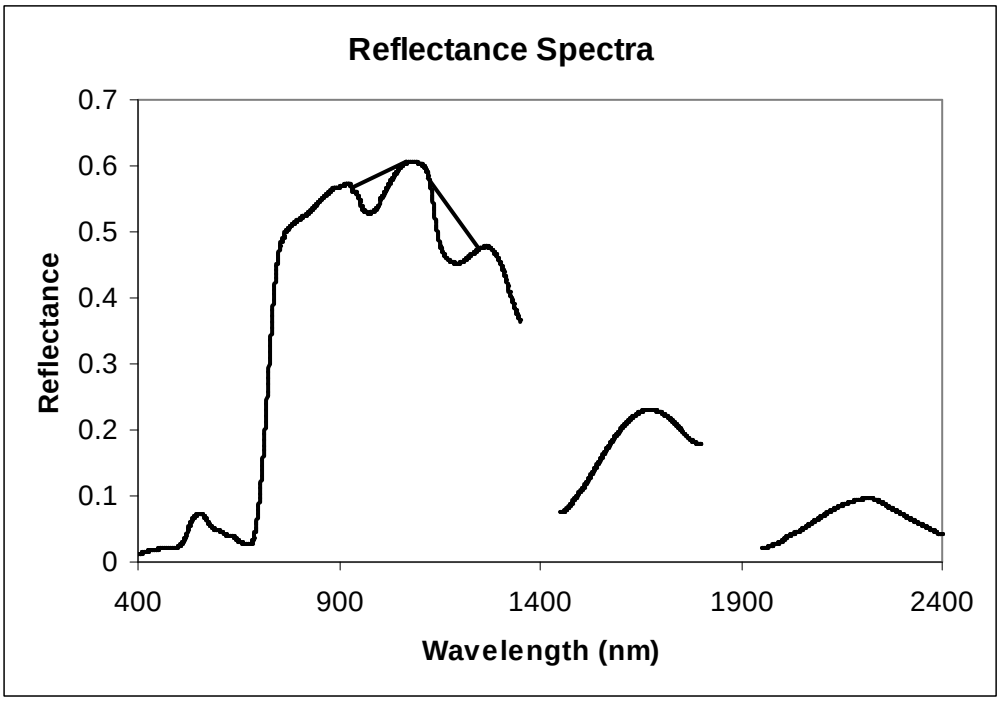

a)

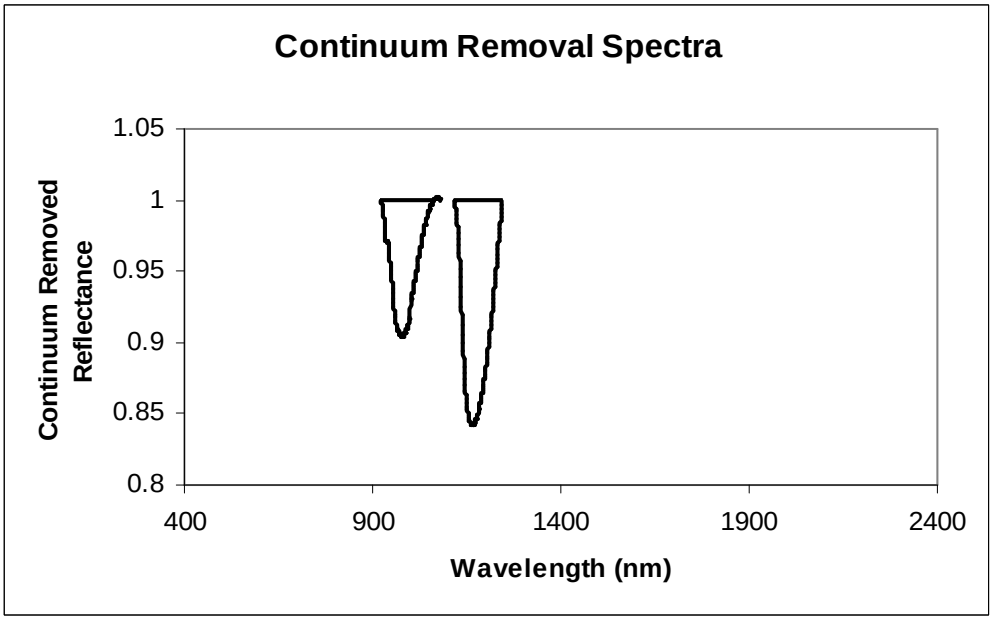

b)

Figure 2. Example spectrum of grassland:

(a) Reflectance spectrum with continuum lines

(b) Continuum removed reflectance spectrum

From the continuum-removed reflectance, the band depth (D) for each channel in the absorption feature was computed by:

$$D = 1 - R' \qquad (9)$$

Where R' is the continuum-removed reflectance (Clark & Roush, 1984).
After computing band depth, maximum band depth, area under the curve, maximum band depth normalized to the area under the curve and area under the curve normalized to the maximum band depth will be calculated according to following formulas:

$$MBD = \max\{D_\lambda\} \qquad (10)$$

$$AUC = \sum D_\lambda \qquad (11)$$

Where λ refers to channels in the absorption feature.
Reflectance spectra of vegetation canopies vary with changing leaf water but remote sensing measurements are also affected by atmospheric absorption, the size of leaf cells, the abundance of other absorbers in the leaf (such as biochemistry), and the fractional area coverage of leaves in heterogeneous landscapes. Therefore, analytical methods for estimation of plant water must overcome any sensitivity to these extraneous factors. Normalization of continuum-removed reflectance spectra minimizes these influences. The normalized band-depth (Dn) at all wavelengths within the continuum-removed absorption feature is calculated by dividing the band-depth of each channel by the band-depth at the band center (Dc):

$$Dn = \frac{D}{Dc} \qquad (12)$$

Where the band center is the minimum of the continuum-removed absorption feature. Variations of Dn with wavelength describe the shape of the absorption feature. Resulting differences in the shapes of absorption features between samples are correlated to foliar water.

3 MATERIALS AND METHOD

3.1 Study area

The first study site is a heterogeneous natural area in the floodplain Millingerwaard along the river Waal in the Netherlands. The floodplain Millingerwaard is part of the Gelderse Poort nature reserve (Figure 3). This is a nature rehabilitation area, meaning that individual floodplains are taken out of agricultural production and are allowed to undergo natural succession. This has resulted in a heterogeneous landscape with river dunes along the river, a large softwood forest in the eastern part along the winter dike and in the intermediate area a mosaic pattern of different succession stages (pioneer, grassland, shrubs). To stimulate the development of a heterogeneous landscape, a low grazing density of 1 animal (e.g., Galloway, Koniks) per 2-4 ha has been chosen. This density allows grazing whole year round and also development of forest is possible. The surface area of water changes over the year. During high floods, the whole floodplain except for the higher parts of the river dunes is flooded. Due to the variability in elevation, some lower areas will be flooded for a relatively long period.

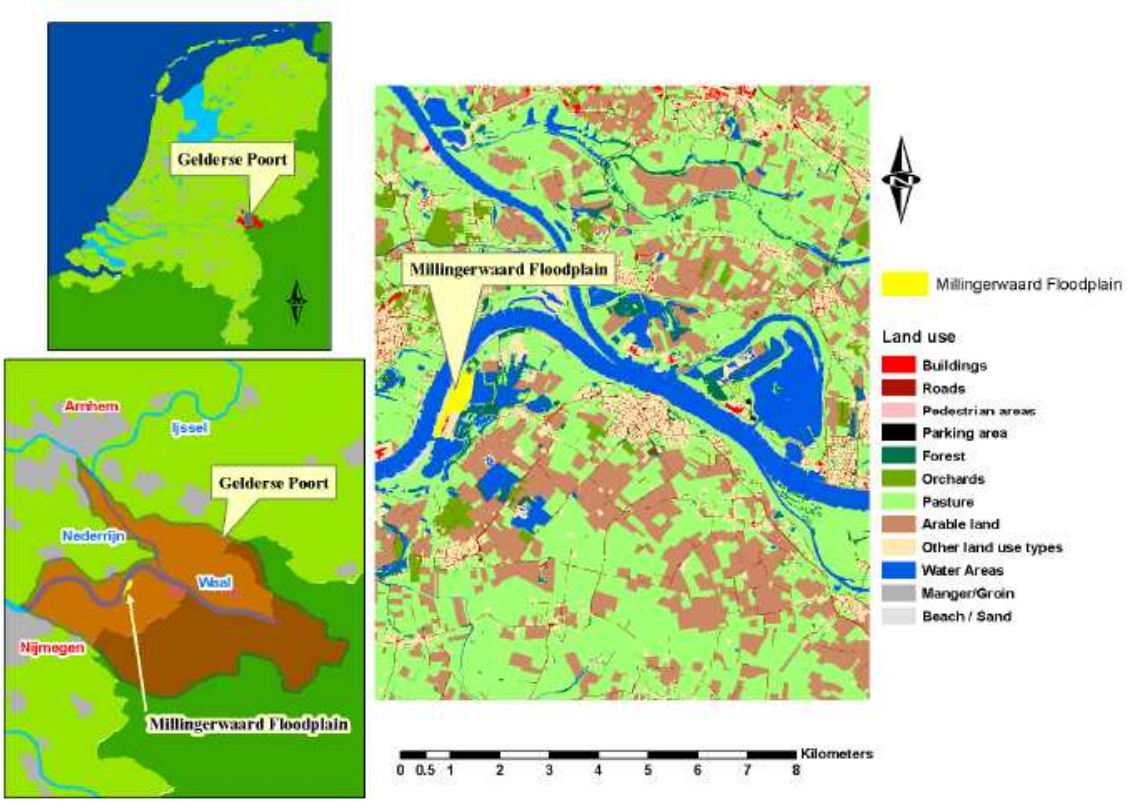

Figure 3.1: Location and current land use for the floodplain Millingerwaard along the river Rhine in the Netherlands.

The second study site is a managed grassland in the Achterhoek in the Netherlands. In the Netherlands several Natura2000 sites have been identified, amongst these is the Korenburgerveen in the Achterhoek near Winterswijk. The Korenburgerveen is a rewetted bog ecosystem with an area of 509 ha consisting of the following habitat types: raised bog, swamp forest, heath land, and extensively used grasslands. In this thesis focus will be on the structure and functioning of the extensively managed grasslands which are located as a buffer zone around the central rewetted bog ecosystem. The grasslands have been gradually taken out of agricultural production and are grazed extensively. Nature managers are interested in the development of the quality of the grasslands over time as under the right conditions valuable habitat types like 'blauwgraslanden' could develop.

Figure 3.2: Location of the Achterhoek in the Netherlands.

3.2 DATA

3.2.1 Field spectroradiometer measurements

On July 28th, 2004, a field campaign with an ASD FieldSpec Pro FR spectroradiometer was performed at site 1 (Millingerwaard). Within 21 square areas of 5 m by 5m centered at each plot 10 spectral measurements were performed, whereby each measurement was the average of 50 readings at the same spot. The area for the spectral measurements (5 m by 5 m) was larger than the one for the destructive sampling (2 m by 2 m). Measurement height was about 1.5 m. Since vegetation height varied for the different plant functional types, the distance between instrument aperture and canopy also varied. A spectralon white reference panel was used for calibration.

For one location only sand was erroneously measured, not the vegetation. Preliminary analysis of the data for this test site showed that four plots, which were influenced by heavy grazing and as a result had a very low but dense grass sward, had a deviating relationship between spectral indices and biomass (Kooistra et al., 2006; Schaepman et al., 2007). These were grouped as a distinct plant functional type and omitted from this study. As a result, 16 plots remained for further analysis. Figure 3.3 gives an overview of all measurements performed on 28 July 2004 over the vegetation plots.

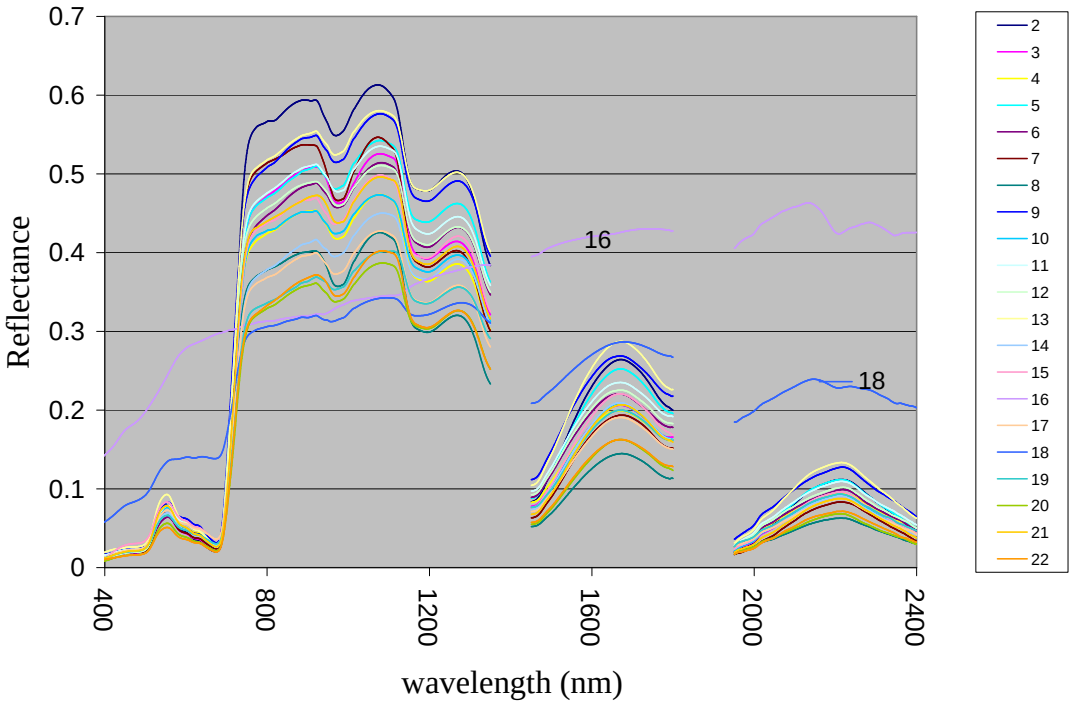

Figure 3.3: Example of 21 FieldSpec measurements in the vegetation plots at Millingerwaard site in 2004

On June 19th, 2005, another field campaign with an ASD FieldSpec Pro FR spectroradiometer was performed at site 1 (Millingerwaard). Within a square area of 20m-20m centered at each plot 12 measurements were performed according to the VALERI sampling scheme (figure 3.4). Every point has a letter associated to it. Each measurement was the average of 15 readings at the same spot. Measurement height was about 1 m above the vegetation.

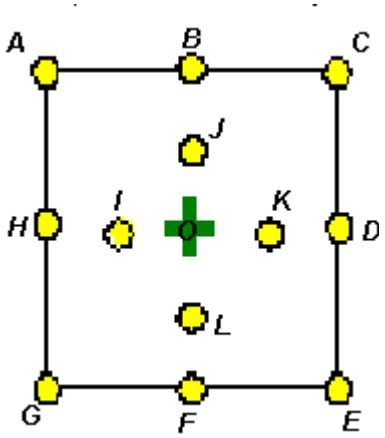

Figure 3.4: Experimental set-up of a sampling plot according to the VALERI-protocol (www.avignon.inra.fr/valeri/).

A description of the vegetation was made for 14 vegetation plots (20 x 20 m) that were also radiometrically characterized. Locations of the plots are shown in Figure 3.5.

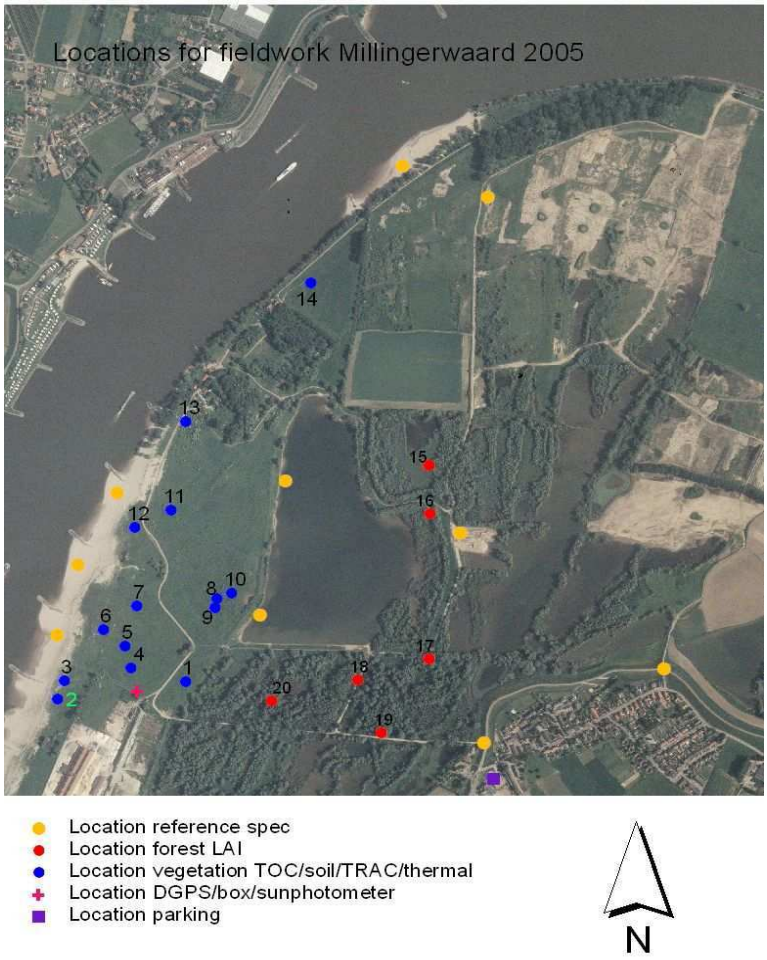

Figure 3.5: Ground based measurements for radiometric corrections and spectral characterization of vegetation within the Millingerwaard floodplain (2005).

After calculating average spectra per plot in 2004 and 2005, the resulting spectra were smoothed using a 15 nm wide moving Savitsky-Golay filter (applying a second order polynomial fit within the window) to reduce instrument noise. Figure 3.6 gives an overview of the measurements performed on 19 June 2005 over the vegetation plots in the Millingerwaard.

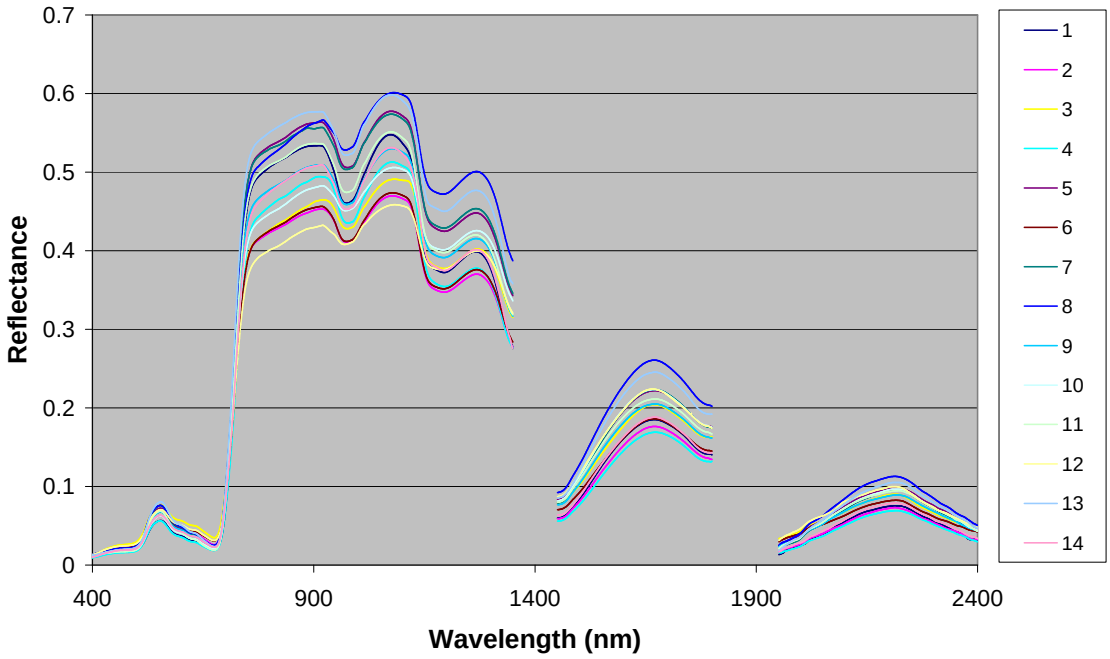

Figure 3.6: Example of 14 FieldSpec measurements in the vegetation plots at the Millingerwaard site in 2005

On June 8th and 9th, 2008, a field campaign with an ASD FieldSpec Pro FR spectroradiometer was performed at test site 2 (Korenburgerveen). Within a square area of 3m by 3m centered at each plot 12 measurements were performed. So, the area for the spectral measurements (3 m by 3 m) was larger than the one for the destructive sampling (2m by 2 m). Measurement height was about 1 m. Since vegetation height varied for the different plant functional types, the distance between instrument aperture and canopy also varied. Figure 3.7 and 3.8 give an overview of the measurements performed on 8 and 9 June 2008 over the vegetation plots. Preliminary analysis of the data for this test site showed that plot 25, which was influenced by heavy grazing and as a result had a very low but dense grass sward, had a deviating relationship between spectral indices and biomass. This was omitted from this study. As a result, 39 plots remained for further analysis. In these three data sets a spectralon white reference panel was used for calibration.

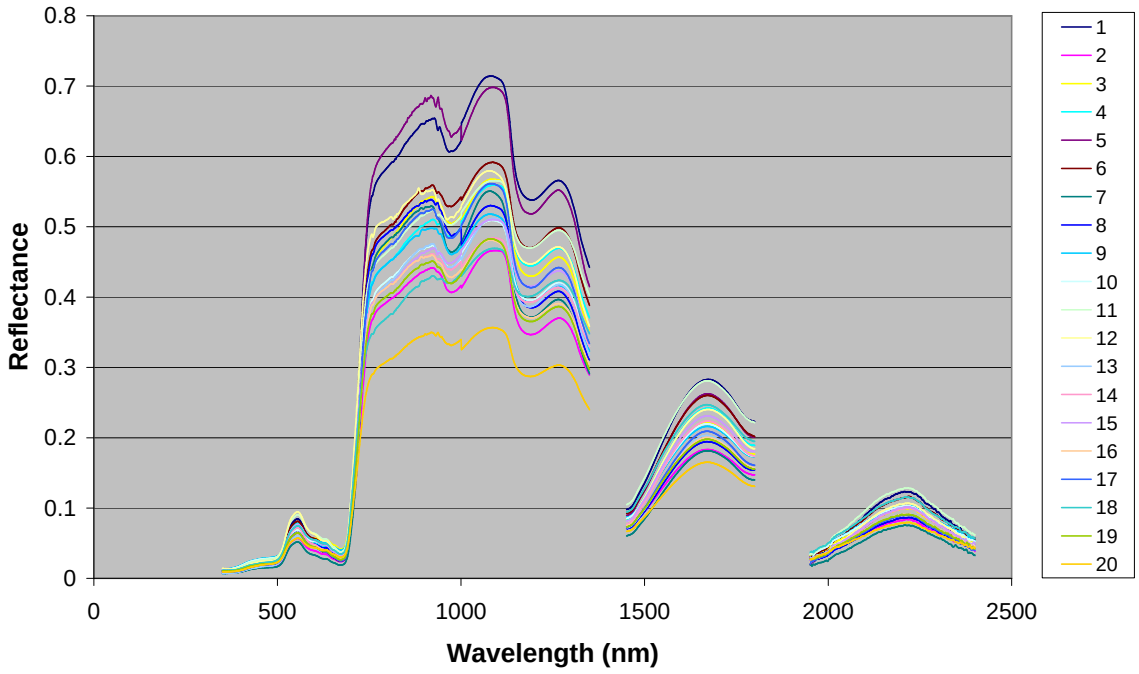

Figure 3.7: Example of first 20 FieldSpec measurements in the vegetation plots at the Korenburgerveen site in 2008.

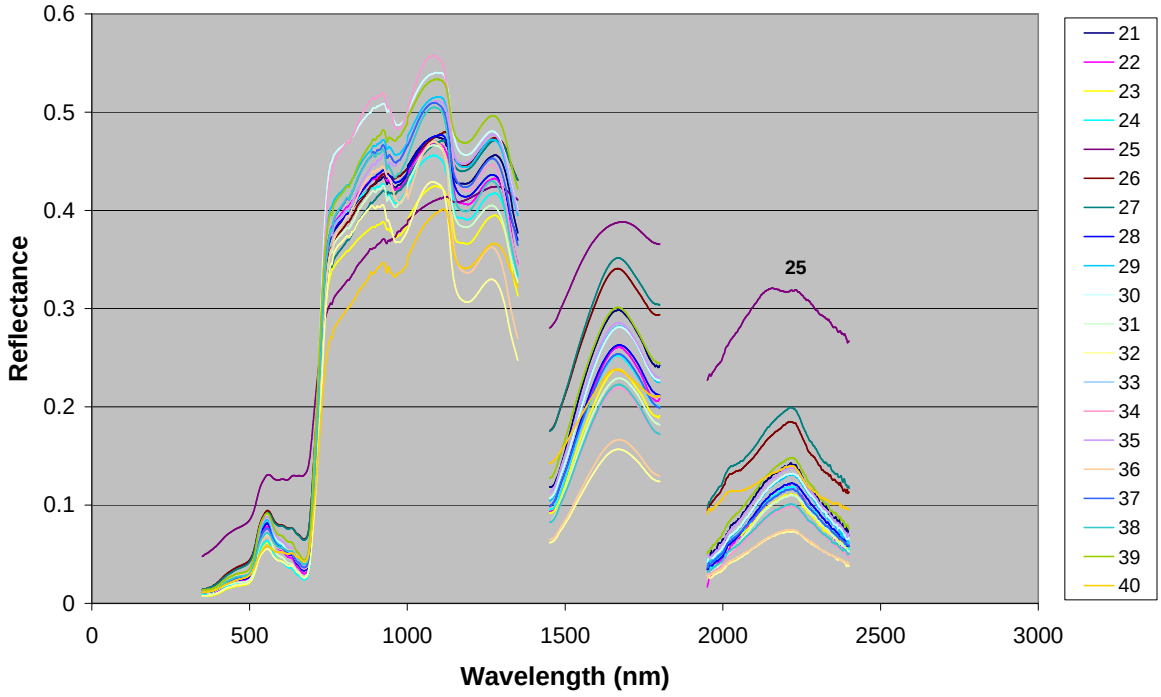

Figure 3.8: Example of second 20 FieldSpec measurements in the vegetation plots at the Korenburgerveen site in 2008.

3.2.2 Biomass

Vegetation biomass was sampled in three subplots with a relatively homogeneous vegetation cover measuring 0.5 x 0.5 m, located within the VALERI-plots. Biomass was clipped at 0.5 cm above the ground level and stored in paper bags. The collected material was weighted for fresh biomass. Subsequently, the average fresh biomass per plot was calculated, and then it was dried for 24 h at 70ºC, After drying for 24 hours at 70°C, vegetation dry matter weight was determined. Subsequently, the average dry biomass per plot was calculated. Unfortunately, no fresh weight was measured in 2004, so canopy water content could not be determined. In order to make comparisons with data set in 2005, we assumed a dry matter content of 30% for all plots based on measurements done in 2005.
Values for the measured fresh and dry weight per sample in 2005 are presented in appendix 3 and average values per plot are presented in appendix 4. Plot 11 and 13 were not harvested in 2005 due to the presence of large shrubs of *Sambucus nigra*. Values for the measured dry weight per plot in 2004 are presented in appendix 5. Values for the measured fresh and dry weight per sample and per plot in the Korenburgerveen in 2008 are presented in appendix 6 and 7.

3.2.3 Airborne image

On July 28th, 2004, airborne imaging spectrometry data were collected from an altitude of 2300 m (a.s.l.) using the HyMap sensor (Integrated Spectronics, Australia) onboard a Dornier DO-228 aircraft operated by the German Aerospace Centre DLR for test site 1 (Millingerwaard). Complete spectra over the range of 450–2480 nm were recorded with a bandwidth of 15–20 nm by 4 spectrographic modules. Each module provided 32 spectral channels giving a total of 128 spectral measurements for each pixel. However, the delivered data contained 126 bands because the first and last bands of the first spectrometer were deleted during pre-processing. Ground resolution of the images was 5 m. The flight line was oriented close to the solar principal plane to minimize directional effects. The HyMap images were geo-atmospherically processed with the modules PARGE and ATCOR4 to obtain geocoded surface reflectance data (Richter & Schlapfer, 2002; Schlapfer & Richter, 2002), approximating hemispherical directional reflectance factors (HDRF) (Schaepman-Strub et al., 2006). Visibility was estimated by combining sun photometer measurements with Modtran4 radiative transfer simulation following the approach of Keller (2001). Finally, spectral signatures were derived for the pixels matching the locations of the 21 plots defined in the field. Again, the four plots with the distinct plant functional type, being influenced by heavy grazing, showed a deviating relationship between spectral indices and biomass. The plot measured as sand with the FieldSpec could be analyzed correctly in the HyMap image. As a result, 17 plots remained for further analysis. Figure 3.9 gives an overview of the 21 spectral signatures using the HyMap image.

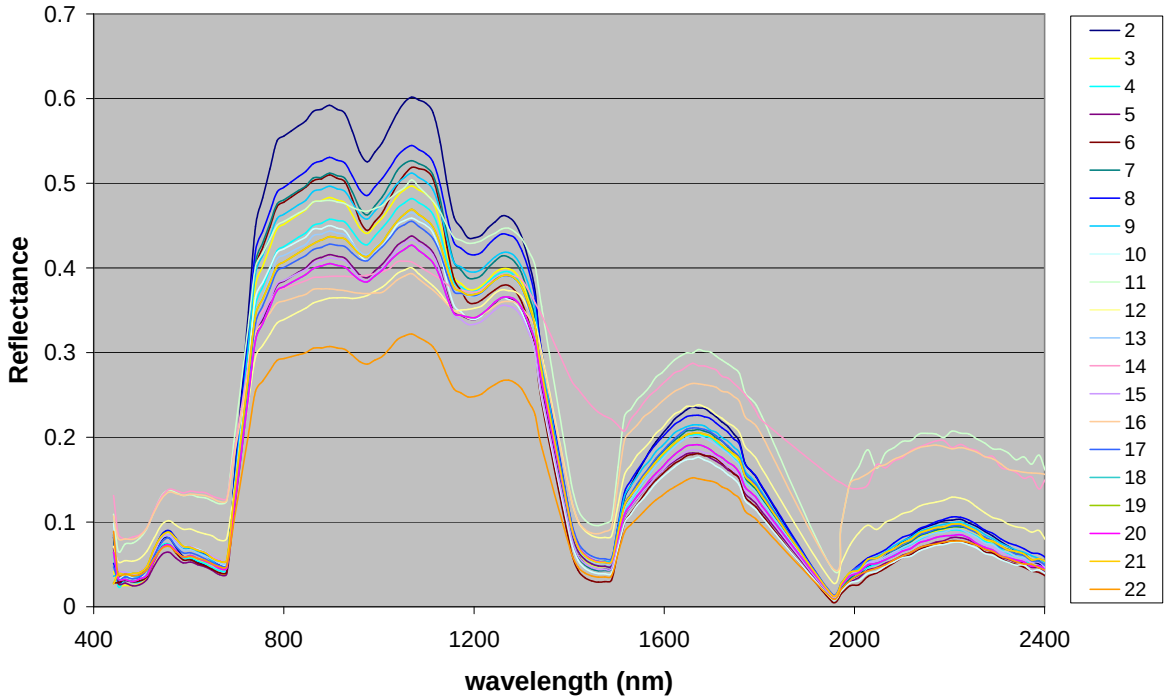

Figure 3.9: Example of 21 spectral signatures as derived from the HyMap image for the Millingerwaard test area in 2004.

3.3 Conceptual model

Several literature sources have published different methods to estimate CWC (Hardisky et al., 1983; Hunt et al. 1989; Penuelas et al. 1993; Gao, 1996; Champagne et al. 2001; Jackson et al. 2004). The thesis aims to adapt the continuum removal technique in the estimation of CWC and compare results based on this technique to those based on WI, NDWI and first derivative of the spectral signature. Figure 3.10 summarizes the approach used for applying the continuum removal technique to the water absorption features in the NIR region to estimate CWC. This conceptual model also included the comparison of derived results with results based on WI, NDWI and first derivative of the spectral signature.

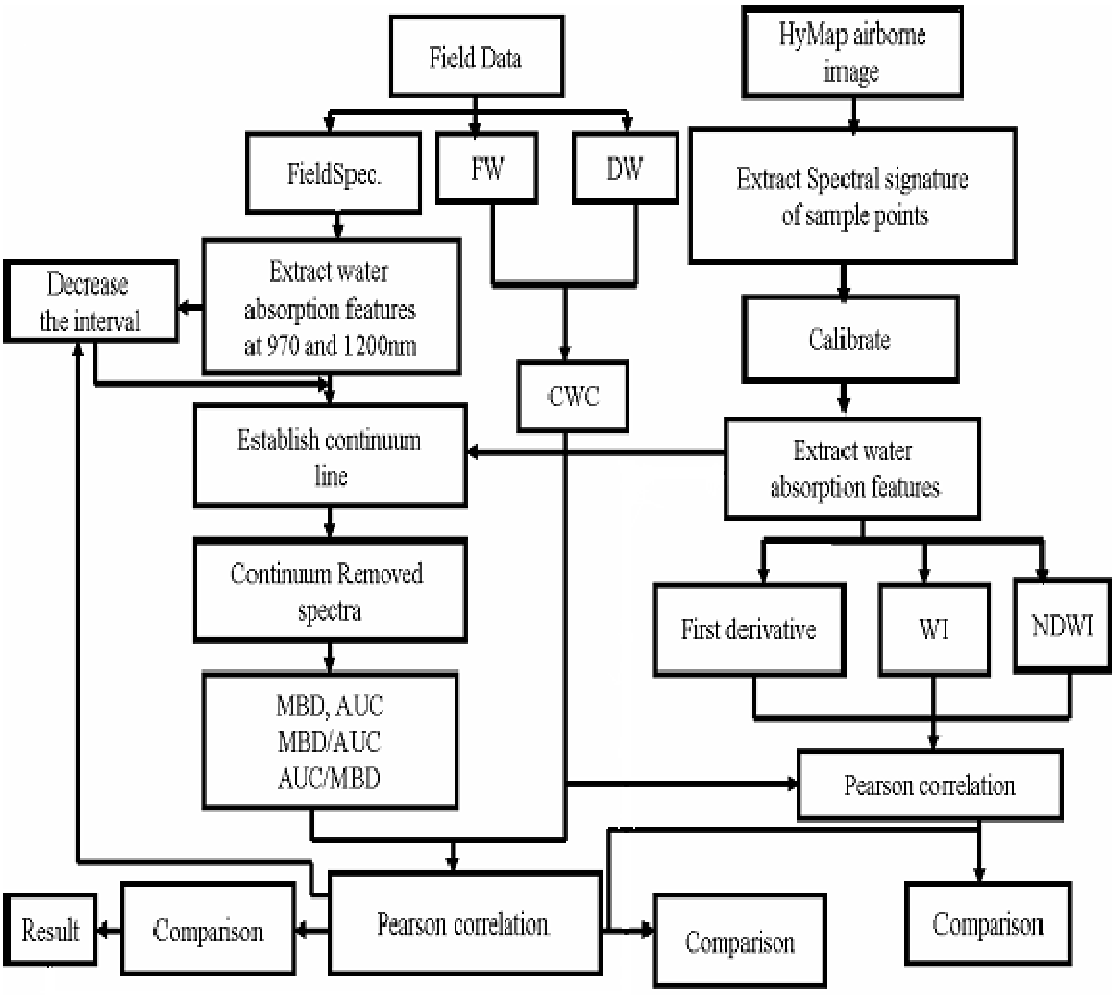

Figure 3.10: Conceptual model indicates connection in research strategies for CWC estimation

3.4 Statistical evaluation of results

The quantity r, called the linear correlation coefficient, measures the strength and the direction of a linear relationship between two variables. In this thesis the correlation coefficient between biomass and continuum removal indices over several intervals, WBI, WBIxxx, NDWI and first derivative is calculated. The mathematical formula for computing r is:

$$r = \frac{n\sum xy - \left(\sum x\right)\left(\sum y\right)}{\sqrt{n\left(\sum x^2\right) - \left(\sum x\right)^2}\sqrt{n\left(\sum y^2\right) - \left(\sum y\right)^2}} \qquad (13)$$

Where n is the number of pairs of data

The value of r is such that -1 < r < +1. The + and – signs are used for positive linear correlations and negative linear correlations, respectively.

The coefficient of determination, r2, is useful because it gives the proportion of the variance (fluctuation) of one variable (FW, DW and CWC) that is predictable from the

indices. It is a measure that allows us to determine how certain one can be in making predictions from a certain model/graph. The coefficient of determination is the ratio of the explained variation to the total variation.

In the next step, it should be checked whether the correlation coefficient is significant. We have set the α level at 0.05. In order to determine if the r value we found with our sample meets that requirement, it will be used a critical value table for Pearson's Correlation Coefficient (see appendix 9). First degrees of freedom (df) must be determined. For a correlation study, the degree of freedom is equal to 2 less than the number of subjects. By using the critical value table it would be found the intersection of α .05 and related degrees of freedom. Then it should be discovered whether there is a statistically significant difference between coefficient of the correlation values between biomass and indices based on the continuum removal technique over different intervals. To reach this purpose the following steps have been followed:

- Make a model for biophysical variables based on each continuum removal index.
- Calculate the estimated biophysical variable based on that model.
- Calculate the difference between the measured and estimated value for biophysical variable per interval (e1, e2, e3 ... e9 at water absorption feature 970 nm and e1, e2, e3… e15 at water absorption 1200 nm).
- Calculate the difference between error of the first interval and the other intervals (e1-e2, e1-e3, e1-e4…).
- Use T-test with α 0.05.

This procedure is used to answer questions such as: is the effect of MBD stronger than AUC for the estimation of biomass? This is used to check the difference between two dependent correlations, thus, from a single sample. This procedure allows seeing if two correlations in a triangle are statistically significantly different. We have to put three correlations in the r1, r2, r3 boxes, respectively. These three correlations have to form a triangle: they must be r_{xy}, r_{zy} and r_{xz}. Give the sample size in the bottom (N2) box. Finally a number of confidence intervals around the difference between the two correlations and p-values are produced (see appendix 10).

4 RESULT

Since the main component of living green vegetation is water, in general fresh weight, dry weight and water content will show a strong association (Rollin and Milton, 1998). So in this thesis the relationship between these three variables and indices was computed and analyzed.

4.1 FW, DW and CWC estimation using Continuum removal indicators

To investigate which interval is suitable for applying the continuum removal technique to the water absorption features in the NIR region it is reasonable to start with broad intervals which include the whole absorption features around 970 nm (920 nm – 1080 nm) and 1200 nm (1080 nm-1280nm). Once the continuum lines around 970 nm and 1200 nm were established separately, continuum-removed spectra were calculated by dividing the original reflectance spectrum by the corresponding reflectance of the continuum line in these two water absorption features.

From the continuum-removed reflectance, the band depth (BD) for each channel in the absorption feature and the band center, the minimum of the continuum-removed absorption feature, were computed.Then it was easy to find the maximum band depth (MBD) and also the area under the continuum (AUC) which is the sum of the band depth in all channels in the absorption feature. Subsequently, maximum band depth was normalized to the area under the continuum and also the area under the continuum was normalized to the maximum band depth. In the further steps, intervals around those water absorption features were decreased by 5 nm at both left and right side, and all the procedures were repeated. Table 4.1 shows one example of all intervals which were considered to apply the continuum removal technique to the water absorption features in the NIR region.

Table 4.1 Continuum start and end point definition for the water absorption feature at 970 nm and 1200 nm in the reflectance spectra of vegetation in Millingerwaard 2005.

	970 nm		1200 nm	
Step	Continuum Line Start (nm)	Continuum Line End (nm)	Continuum Line Start (nm)	Continuum Line End (nm)
1	920	1080	1080	1280
2	925	1075	1085	1275
3	930	1070	1090	1270
4	935	1065	1095	1265
5	940	1060	1100	1260
6	945	1055	1105	1255
7	950	1050	1110	1250
8	955	1045	1115	1245
9	960	1040	1120	1240
10			1125	1235
11			1130	1230
12			1135	1225
13			1140	1220
14			1145	1215
15			1150	1210

4.1.1 Continuum Removal Indices of FieldSpec Measurement

Since fresh weight, dry weight and canopy water content are associated, it makes sense to relate indices based on the water absorption features also with dry weight for the FieldSpec measurements in 2004 (fresh weight and water content were not measured).
Figure 4.1 shows the results of the coefficient of determination between dry weight and indices based on the continuum removal technique (MBD, AUC, MBD/AUC and AUC/MBD) over different intervals at water absorption features 970 nm and 1200 nm of vegetation plots measured with the ASD FieldSpec pro in Millingerwaard site in 2004.
Figure 4.1 (a) shows a linear pattern. The maximum value of the coefficient of determination for MBD and AUC/MBD is 0.1, for AUC it is 0.08 and for MBD/AUC it is 0.16. All are located in the interval 960 nm to 1040 nm of the spectral signature. The minimum value of the coefficient of determination for MBD/AUC and AUC/MBD is 0.0 and for MBD it is 0.05 and for AUC it is 0.04. These are located in the interval 920 nm to 1080 nm of the spectral signature. This graph also shows some fluctuations in the coefficient of determination between DW and MAB/AUC and AUC/MBD over different intervals.
Figure 4.2 (b) shows that the coefficient of determination between dry weight and MBD/AUC and AUC/MBD is zero over all intervals, The coefficient of determination between dry weight and MBD and AUC is 0.065 and is constant till interval 1125 nm to 1235 nm, then it increases to 0.09.

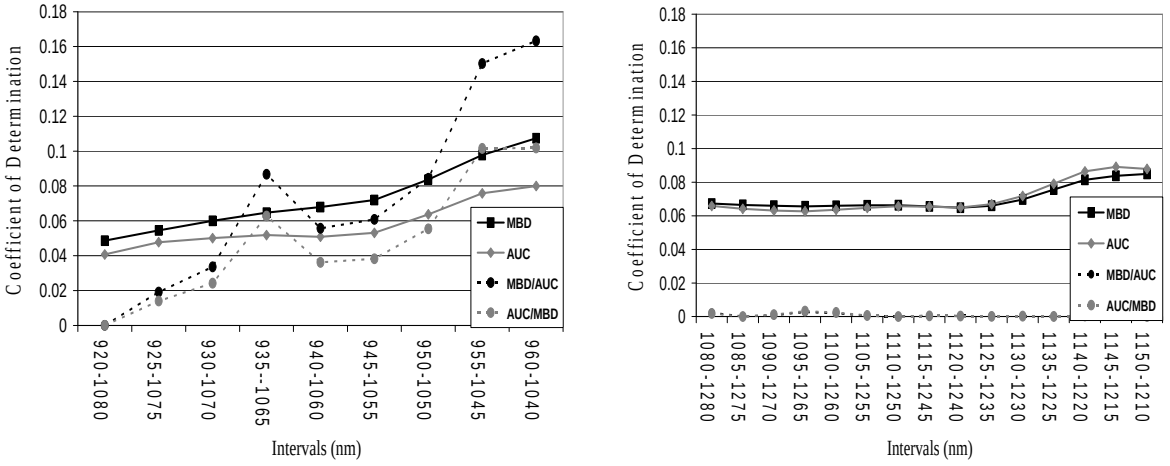

(a) (b)

Figure 4.1 Comparison of coefficient of determination between dry weight and continuum removal indices based on FieldSpec measurements in 2004 in Millingerwaard site, considering different intervals

(a) At water absorption feature 970 nm.

(b) At water absorption feature 1200 nm

Now it should be checked whether the correlation coefficient of DW and these indices over different intervals is significant. In this data set for 2004 degrees of freedom would be 14. By using the critical value table (see appendix 9) it would be found the intersection of α .05 and 14 degrees of freedom. The value found at the intersection (.497) is the minimum correlation coefficient r that we would need to confidently state 95 times out of a hundred that the relationship we found with my 16 pairs exists in the population from which they were drawn.

Table 4.2 and 4.3 show that all absolute values of the correlation coefficient are less than 0.497. So, we fail to reject the null hypotheses. There is not a statistically significant relationship between DW and indices based on the continuum removal technique at the water absorption features in the NIR region on the FieldSpec measurements in the Millingerwaard site in 2004.

Table 4.2 Correlation coefficient of DW and continuum removal indices at the water absorption feature 970 nm based on FieldSpec measurements in 2004 in Millingerwaard site.

Interval (nm)	r(DW, MBD)	r(DW,AUC)	r(DW,MBD/AUC)	r(DW,AUC/MBD)
920-1080	0.220	0.202	-0.007	-0.007
925-1075	0.233	0.219	-0.138	0.118
930-1070	0.245	0.224	-0.183	0.156
935-1065	0.254	0.228	-0.294	0.251
940-1060	0.261	0.226	-0.236	0.190
945-1055	0.268	0.231	-0.247	0.196
950-1050	0.289	0.252	-0.291	0.235
955-1045	0.313	0.275	-0.388	0.319
960-1040	0.328	0.283	-0.404	0.319

Table 4.3 Correlation coefficient of DW and continuum removal indices at the water absorption feature 1200 nm based on FieldSpec measurements in 2004 in Millingerwaard site.

Interval (nm)	r(DW,MBD)	r(DW,AUC)	r(DW,MBD/AUC)	r(DW,AUC/MBD)
1080-1280	0.259	0.257	-0.048	0.043
1085-1275	0.258	0.253	-0.005	-0.001
1090-1270	0.257	0.251	0.029	-0.034
1095-1265	0.256	0.250	0.052	-0.057
1100-1260	0.257	0.252	0.045	-0.049
1105-1255	0.257	0.254	0.022	-0.026
1110-1250	0.258	0.256	-0.007	0.004
1115-1245	0.256	0.256	-0.023	0.021
1120-1240	0.255	0.255	-0.020	0.018
1125-1235	0.257	0.259	-0.013	0.011
1130-1230	0.264	0.268	-0.018	0.017
1135-1225	0.275	0.281	-0.008	0.008
1140-1220	0.285	0.294	-0.017	0.017
1145-1215	0.290	0.299	-0.031	0.031
1150-1210	0.292	0.297	0.001	-0.002

Figure 4.2 shows the results of the coefficient of determination between biomass and indices based on the continuum removal technique over several intervals at the water absorption feature 970 nm of vegetation plots measured with the ASD FieldSpec pro at the Millingerwaard site in 2005. Graphs in figure 4.2a, b and c, which are related to fresh weight, dry weight and canopy water content, follow exactly the same pattern. These three graphs show that biomass (FW, DW, and CWC) has the highest correlation with MBD and AUC in the first interval (920 nm – 1080 nm) and with MBD/AUC and AUC/MBD in the second interval (925 nm to 1075 nm). Also they show that the biomass and indices based on the continuum removal technique have the lowest correlation in the last interval around the water absorption feature at 970 nm (960 nm – 1040 nm). In this way it is visible through these graphs that CWC has the highest value in all intervals around the water absorption feature at 970 nm in comparison with FW and DW. DW has the lowest r^2.

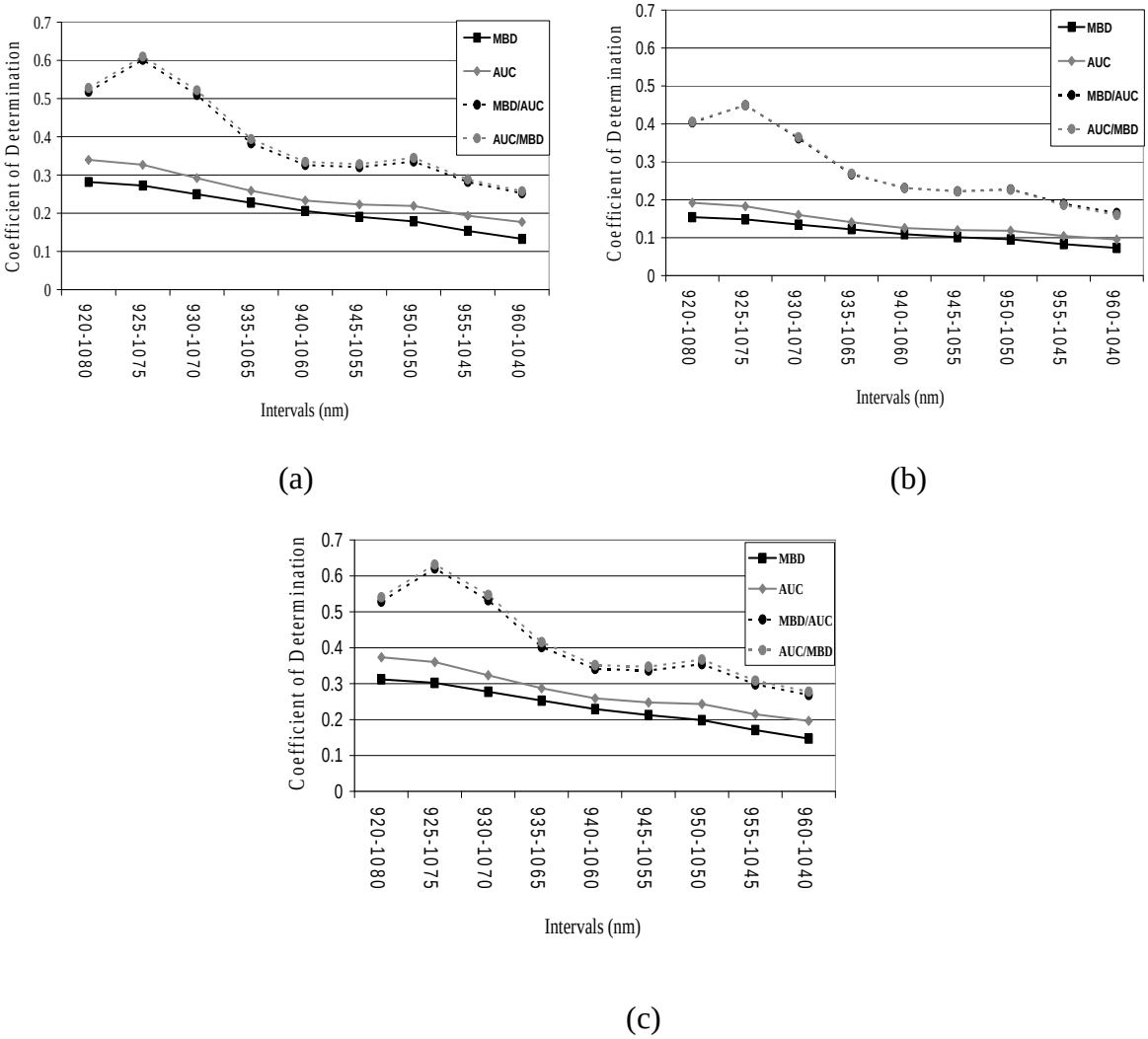

Figure 4.2 Coefficient of determination between biomass and continuum removal indices in different intervals at the water absorption feature 970nm in Millingerwaard in 2005.

a) Fresh weight

b) Dry weight

c) Canopy water content

Figure 4.3 shows results of the coefficient of determination between biomass and indices based on the continuum removal technique over several intervals at the water absorption feature 1200 nm of vegetation plots measured with the ASD FieldSpec pro in the Millingerwaard site in 2005.

In general, graphs in figure 4.3a, b and c, which are related to fresh weight, dry weight and canopy water content, show that the coefficient of determination between CWC and indices is almost the same as the coefficient of determination between FW and those indices are higher than those for DW. The MBD and AUC in these three graphs have a constant value for the coefficient of determination in initial intervals and then follow a decreasing pattern. The other two follow a more cosinusoidal pattern.

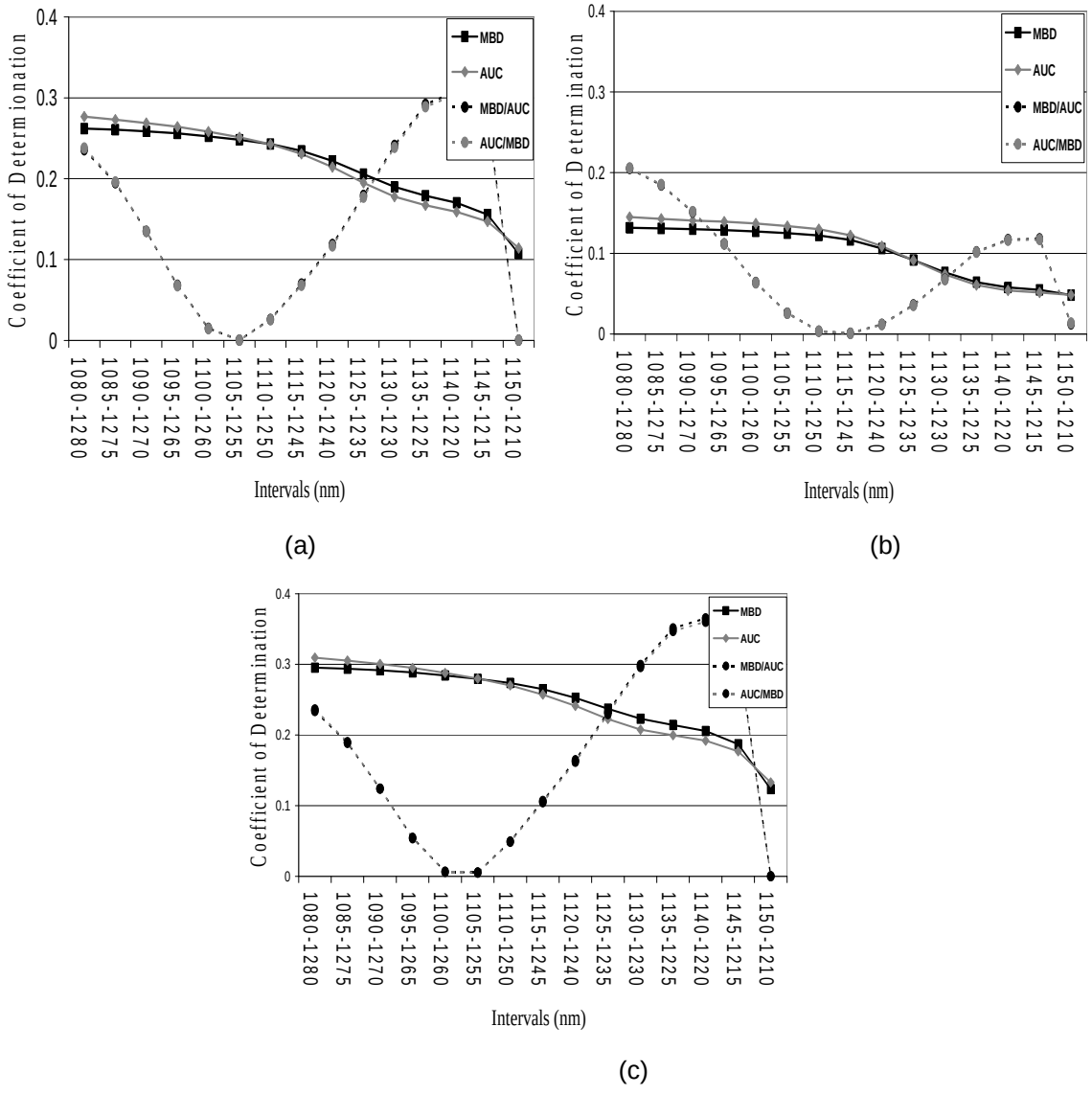

Figure 4.3 Coefficient of determination between biomass and continuum removal indices in different intervals at the water absorption feature 1200nm in Millingerwaard in 2005.

a) Fresh weight

b) Dry weight

c) Canopy water content

Since in this data set 12 samples are available, so the degrees of freedom would be 10. By using the critical value table a value is 0.576 at the intersection of α 0.05 and 10 degrees of freedom. Table 4.5 shows that all absolute values of the correlation coefficient of CWC with MBD are less than 0.576. So, we fail to reject the null hypotheses. There is not a statistically significant relationship between CWC and MBD at the water absorption feature 970 nm based on FieldSpec measurements in the Millingerwaard site in 2005. However, the absolute values for the correlation coefficient of CWC with AUC in the three first intervals which have been highlighted are more than 0.576 and also for MBD/AUC and AUC/MBD in seven intervals they are more than 0.567. Therefore in these intervals we reject the null hypothesis which means there is a statistically significant relationship between CWC and AUC, MBD/AUC and AUC/MBD, respectively, in water absorption feature 970 nm on FieldSpec measurement in this data set.

Table 4.4 shows that the correlation coefficient of CWC with MBD and AUC is statistically not significant in any of the intervals. The correlation coefficient of CWC with MBD/AUC and also AUC/MBD is statistically significant in only two intervals.

Table 4.4 Correlation coefficient of CWC and continuum removal indices at the water absorption feature 970 nm based on FieldSpec measurements in 2005 in Millingerwaard site

Interval	r(CWC,MBD)	r(CWC, AUC)	r(CWC, MBD/AUC)	r(CWC,AUC/MBD)
920-1080	0.559	**0.611**	**-0.727**	**0.735**
925-1075	0.550	**0.600**	**-0.788**	**0.795**
930-1070	0.527	**0.569**	**-0.730**	**0.740**
935-1065	0.503	0.536	**-0.634**	**0.645**
940-1060	0.479	0.509	**-0.584**	**0.593**
945-1055	0.461	0.498	**-0.580**	**0.589**
950-1050	0.446	0.493	**-0.595**	**0.606**
955-1045	0.413	0.464	-0.546	0.555
960-1040	0.384	0.443	-0.518	0.527

Table 4.5 Correlation coefficient of CWC and continuum removal indices at the water absorption feature 1200 nm based on FieldSpec measurements in 2005 in Millingerwaard site

Interval(nm)	r(CWC,MBD)	r(CWC, AUC)	r(CWC, MBD/AUC)	r(CWC,AUC/MBD)
1080-1280	0.543	0.556	-0.484	0.486
1085-1275	0.542	0.553	-0.434	0.436
1090-1270	0.540	0.548	-0.352	0.352
1095-1265	0.537	0.543	-0.234	0.232
1100-1260	0.533	0.536	-0.081	0.078
1105-1255	0.529	0.529	0.072	-0.074
1110-1250	0.523	0.520	0.222	-0.221
1115-1245	0.515	0.507	0.327	-0.324
1120-1240	0.503	0.491	0.405	-0.402
1125-1235	0.487	0.472	0.482	-0.479
1130-1230	0.472	0.456	0.547	-0.544
1135-1225	0.463	0.447	**0.592**	**-0.589**
1140-1220	0.453	0.438	**0.604**	**-0.600**
1145-1215	0.432	0.420	0.564	-0.559
1150-1210	0.351	0.365	-0.012	-0.008

Figure 4.4 shows results of the coefficient of determination between biomass and indices based on continuum removal technique over several intervals at the water absorption feature 970 nm of vegetation plots measured with the ASD FieldSpec at the Korenburgerveen site in 2008.

In general figure 4.4a, b and c, which are related to fresh weight, dry weight and canopy water content, show that MBD and AUC have a stronger correlation with biomass (FW, DW) and CWC than MBD/AUC and AUC/MBD. Also it is visible that the coefficient of determination between indices based on the continuum removal technique and CWC and FW by following the same pattern are approximately the same and higher than those for DW.

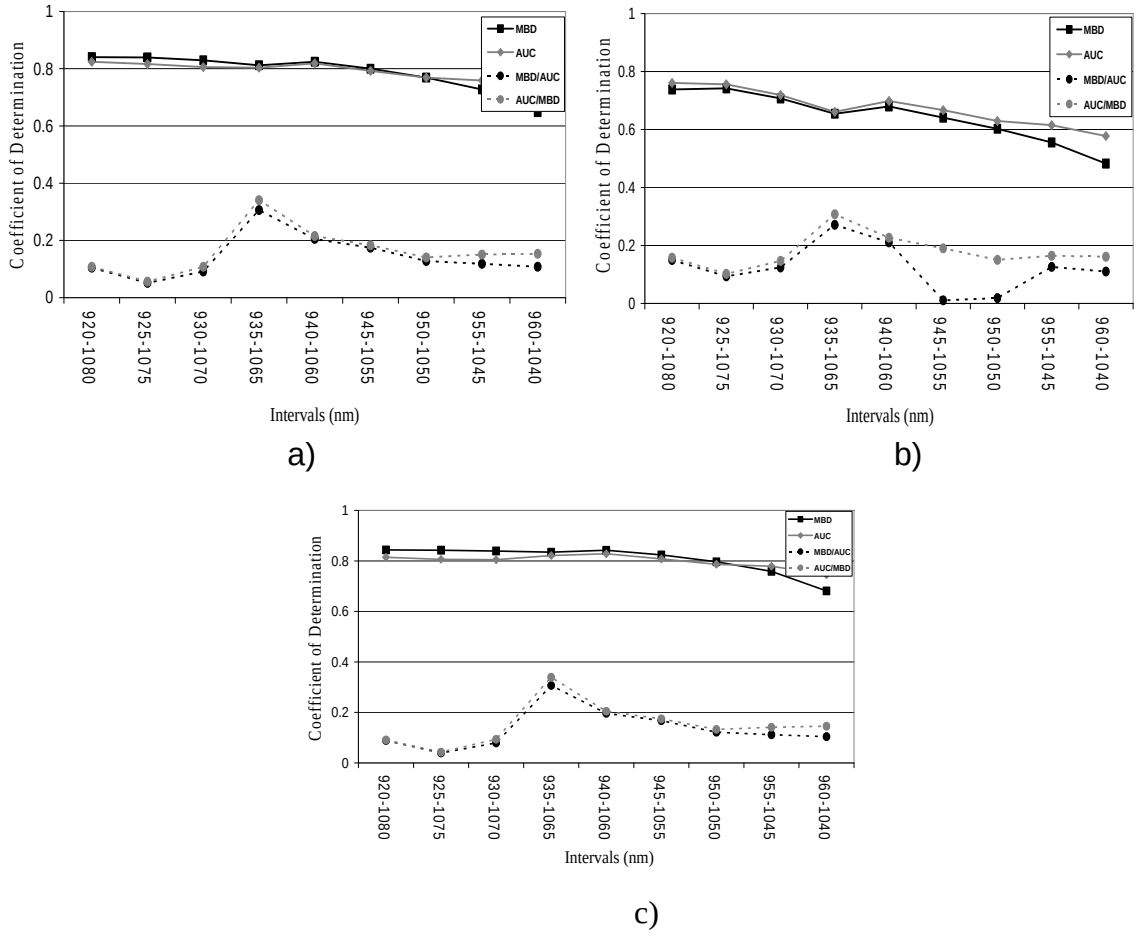

Figure 4.4 Coefficient of determination between biomass and continuum removal indices in different intervals at the water absorption feature 970nm in the Korenburgerveen in 2008.

a) Fresh weight

b) Dry weight

c) Canopy water content

Figure 4.5 shows results of the coefficient of determination between biomass and indices based on the continuum removal technique over several intervals at the water absorption feature 1200 nm of vegetation plots measured with the ASD FieldSpec at the Korenburgerveen site in 2008. In general it shows that the coefficient of determination between biomass and MBD and AUC are almost constant over different intervals of the spectral signature. This figure also shows that the correlation between biomass and MBD/AUC and AUC/MBD is increasing in most of the intervals except in the last few intervals. It is visible through these graphs that the coefficient of determination between FW and indices follows the same value as the coefficient of determination between CWC and the indices.

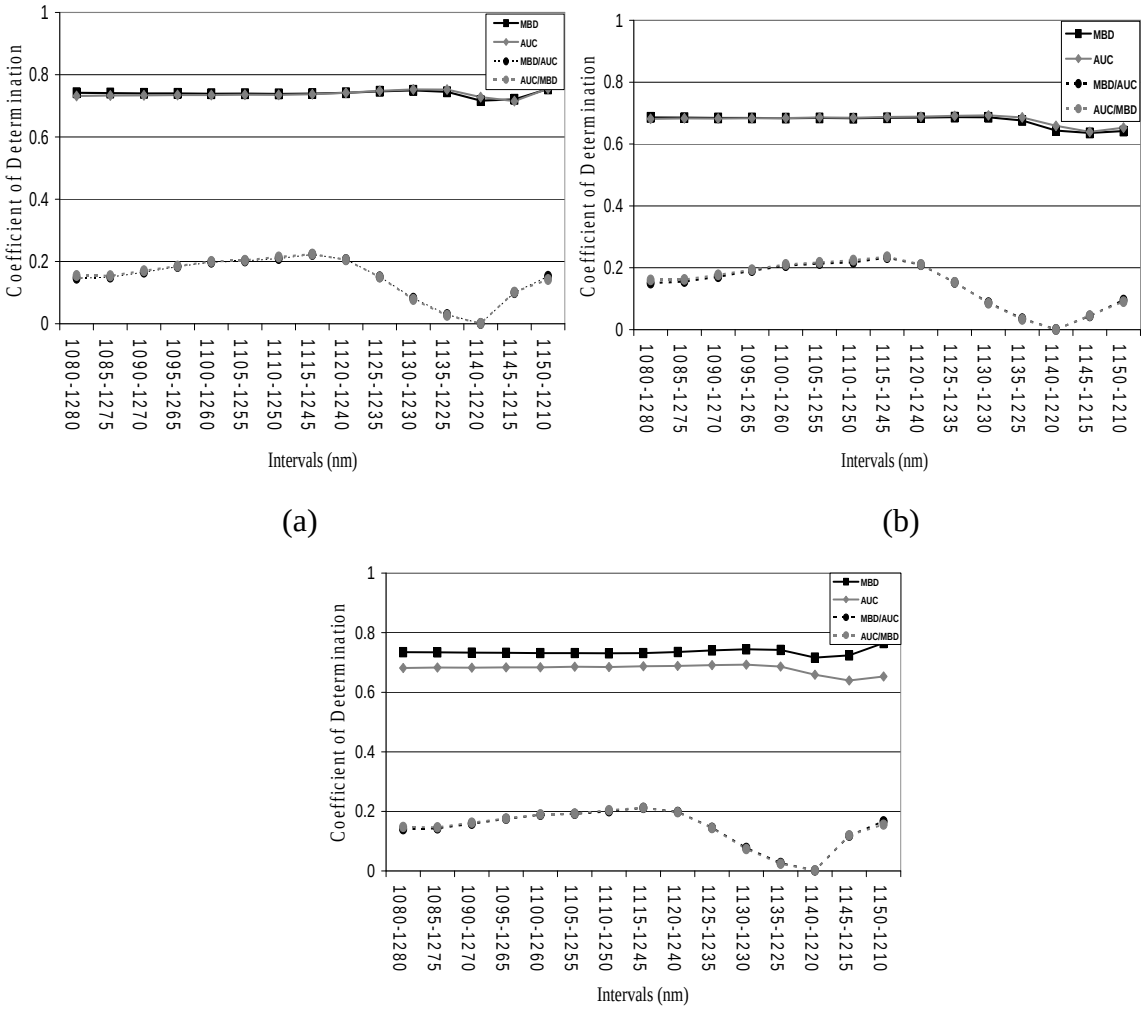

Figure 4.5 Coefficient of determination between biomass and continuum removal indices in different intervals at the water absorption feature 1200nm in the Korenburgerveen in 2008.

a) Fresh weight

b) Dry weight

c) Canopy water content

Since in this data set 39 samples are available, the degrees of freedom would be 37. By using the critical value table a value is found of 0.325 at the intersection of α .05 and 37 degrees of freedom. Table 4.6 shows that all absolute values of the correlation coefficient of CWC with MBD and AUC are more than 0.325. The absolute values for the correlation coefficient of CWC with MBD/AUC and AUC/MBD only in some intervals which have been highlighted is more than 0.325. Therefore in these intervals we reject the null hypothesis which means there is a statistically significant relationship between CWC and AUC and MBD/AUC and AUC/MBD at the water absorption feature 970 nm based on FieldSpec measurements in this data set. Table 4.7 shows that the correlation coefficient of CWC with MBD and AUC is statistically significant in all intervals and the correlation coefficient of CWC with MBD/AUC and also AUC/MBD in only three intervals is statistically not significant.

Table 4.6 Correlation coefficients of CWC and continuum removal indices at the water absorption feature 970 nm based on FieldSpec measurements in 2008 in the Korenburgerveen site.

Interval (nm)	r(CWC,MBD)	r(CWC, AUC)	r(CWC, MBD/AUC)	r(CWC,AUC/MBD)
920-1080	**0.918**	**0.903**	-0.297	0.301
925-1075	**0.918**	**0.898**	-0.198	0.207
930-1070	**0.916**	**0.897**	-0.281	0.306
935-1065	**0.914**	**0.906**	**-0.554**	**0.582**
940-1060	**0.918**	**0.910**	**-0.443**	**0.452**
945-1055	**0.908**	**0.899**	**-0.409**	**0.418**
950-1050	**0.892**	**0.887**	**-0.349**	**0.364**
955-1045	**0.871**	**0.883**	**-0.334**	**0.376**
960-1040	**0.825**	**0.863**	-0.322	**0.381**

Table 4.7 Correlation coefficients of CWC and continuum removal indices at the water absorption feature 1200 nm based on FieldSpec measurements in 2008 in the Korenburgerveen site.

Interval (nm)	r(CWC,MBD)	r(CWC, AUC)	r(CWC, MBD/AUC)	r(CWC,AUC/MBD)
1080-1280	**0.857**	**0.850**	**-0.375**	**0.384**
1085-1275	**0.857**	**0.851**	**-0.378**	**0.383**
1090-1270	**0.856**	**0.852**	**-0.398**	**0.403**
1095-1265	**0.856**	**0.852**	**-0.419**	**0.420**
1100-1260	**0.855**	**0.852**	**-0.434**	**0.436**
1105-1255	**0.855**	**0.853**	**-0.438**	**0.439**
1110-1250	**0.855**	**0.852**	**-0.447**	**0.459**
1115-1245	**0.855**	**0.854**	**-0.460**	**0.461**
1120-1240	**0.857**	**0.857**	**-0.446**	**0.444**
1125-1235	**0.861**	**0.861**	**-0.381**	**0.379**
1130-1230	**0.863**	**0.864**	-0.278	0.271
1135-1225	**0.861**	**0.865**	-0.164	0.155
1140-1220	**0.846**	**0.852**	0.044	-0.051
1145-1215	**0.851**	**0.846**	**0.344**	**-0.346**
1150-1210	**0.875**	**0.874**	**0.408**	**-0.394**

4.1.2 Continuum Removal Indices of HyMap image in 2004

Figure 4.6 shows the coefficient of determination between DW and indices based on the continuum removal technique in two different intervals (928.25nm-1084.05nm and 958.95nm – 1038.45nm) around the water absorption feature at 970 nm of the HyMap image in 2004. Since some sample plots had been located exactly at the border of two pixels of the images. I extracted spectral signature one time by only considering one pixel (a) and next time by considering 3 by 3 pixels (b). Figure 4.6a and b indicate that DW has a higher correlation with MBD and AUC when the whole absorption feature has been included to apply the continuum removal technique than when only some part of the water absorption feature has been included. On the other hand they show DW has higher correlation with MBD/AUC and AUC/MBD in narrower interval around the water absorption feature at 970 nm. Figure 4.6b shows that the coefficient of determination between DW and MBD/AUC and AUC/MBD is much higher than those in figure 4.6a.

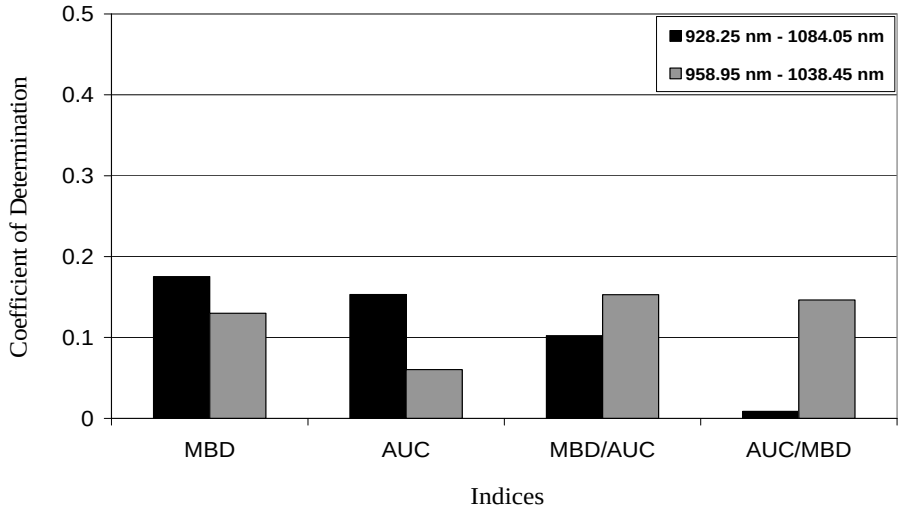

(a)

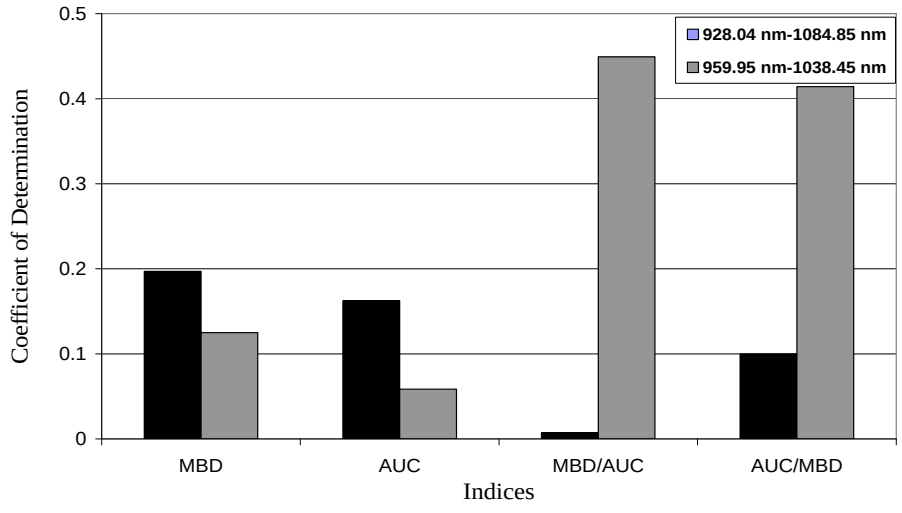

(b)

Figure 4.6 Coefficient of Determination between DW and continuum removal indices for two different intervals around 970 nm for the HyMap image in 2004.

(a) Considering only 1 pixel

(b) Considering 3 by 3 pixels

Figure 4.7 shows the coefficient of determination between DW and indices based on the continuum removal technique in two different intervals (1084.05nm-1286.95nm and 1158.05nm – 1230.25nm) around the water absorption feature at 1200 nm of the HyMap image in 2004 by extracting the spectral signature of one pixel (a) and 3 by 3 pixels (b). Figure 4.7a shows that the coefficient of determination between DW and MBD and AUC are almost the same in both intervals and are about 0.1. The values for MBD/AUC and AUC/MBD are higher for the broader interval. The maximum value is 0.13 for the AUC in the narrower interval and MBD/AUC and AUC/MBD in the broader interval. Figure 4.7b shows that in general the correlation between DW and continuum removal indices in broader intervals is higher than in narrower intervals when 3 by 3 pixels are considered to extract the spectral signature and the maximum value is 0.13 which is related to MBD/AUC and AUC/MBD.

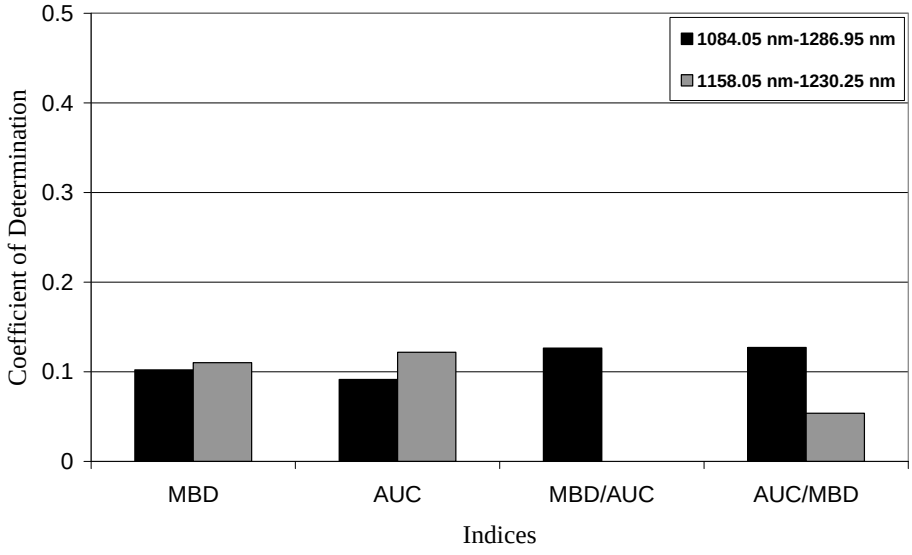

(a)

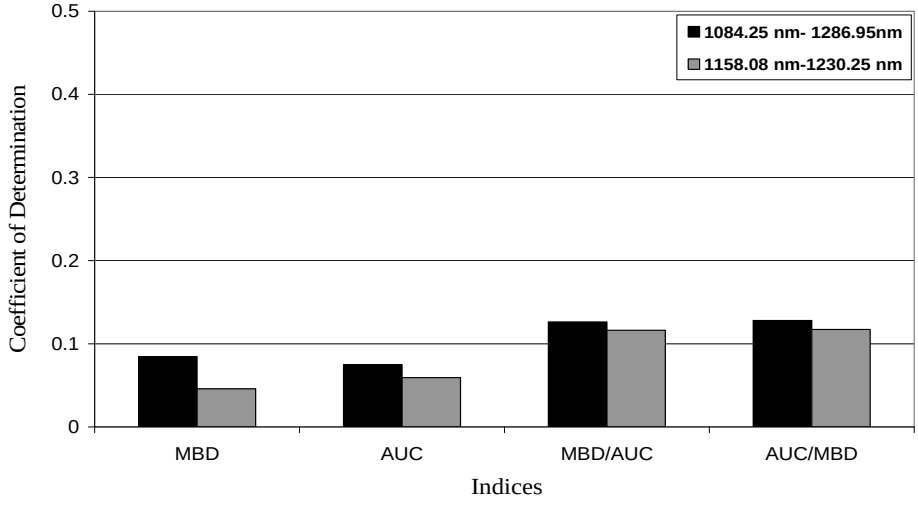

(b)

Figure 4.7 Coefficient of Determination between DW and continuum removal indices in two different intervals around 1200 nm for the HyMap image in 2004.

(a) Considering only 1 pixel

(b) Considering 3 by 3 pixels

In this data set, the degrees of freedom would be 15. So a value of 0.482 is found at the intersection of α 0.05 and 15 degrees of freedom. Table 4.9 and 4.10 show the correlation coefficients of DW with continuum removal indices around water absorption features 970 nm and 1200 nm. All values in table 4.8 are less than 0.482. We would fail to reject our null hypotheses: There is not a statistically significant relationship between DW and indices based on the continuum removal technique at the water absorption features 970 nm and 1200 nm in the HyMap image of the Millingerwaard site in 2004 when only one pixel has been considered to extract the spectral signature. Table 4.9 shows there is a statistically significant relationship between DW and MBD/AUC and AUC/MBD at water absorption feature 970 nm in the interval 958.95 nm to 1038.45 nm when using 3 by 3 pixels per plot.

Table 4.8 Correlation coefficient of DW and continuum removal indices at water absorption feature 970 nm and 1200 nm based on the HyMap image considering only one pixel in Millingerwaard site in 2004.

Interval (nm)	r(DW,MBD)	r(DW, AUC)	r(DW, MBD/AUC)	r(DW,AUC/MBD)
928.25-1084.05	0.419	0.391	-0.320	0.093
958.95-1038.45	0.361	0.246	0.391	-0.382
1084.05-1286.95	0.320	0.302	0.355	-0.356
1158.05-1230.25	0.332	0.349	-0.222	0.232

Table 4.9 Correlation coefficient of DW and continuum removal indices at water absorption features 970 nm and 1200 nm based on the HyMap image considering 3 by 3 pixels in Millingerwaard site in 2004.

Interval (nm)	r(DW,MBD)	r(DW, AUC)	r(DW, MBD/AUC)	r(DW,AUC/MBD)
928.25-1084.05	0.444	0.403	-0.086	0.316
958.95-1038.45	0.354	0.242	**0.670**	**-0.644**
1084.05-1286.95	0.291	0.274	0.355	-0.358
1158.05-1230.25	0.214	0.243	-0.341	0.342

4.2 Water Band Index

Table 4.10 shows the correlation coefficient and the coefficient of determination between WBI and biophysical variables in each dataset. This relationship in the 2004 datasets for both FieldSpec and HyMap (1pixel and 3*3 pixels) is not statistically significant with α 0.05 and 14 degrees of freedom in the FieldSpec data set and 15 degrees of freedom in the HyMap dataset. Results in 2005 show that the relationship between WBI and both FW and CWC are significant with α .05 and 10 degrees of freedom. For the 2008 FieldSpec data, the correlation coefficient between WBI and these three biophysical variables are statistically significant with α .05 and 37 degrees of freedom.

Table 4.10 Correlation coefficient of biomass and WBI in three FieldSpec and one HyMap dataset.

Data set in:	**df**	**p-value**	**Biomass**	**r(WI , biomass)**	**R2(WI , biomass)**
2004 (FieldSpec.)	14	0.497	DW	0.406	0.165
(HyMap-1pixel)	15	0.482	DW	0.401	0.161
(HyMap-3*3pixels)				0.423	0.179
2005 (FieldSpec.)	10	0.576	FW	**0.607**	0.368
			DW	0.478	0.228
			CWC	**0.630**	0.397
2008 (FieldSpec.)	37	0.325	FW	**0.888**	0.789
			DW	**0.811**	0.658
			CWC	**0.896**	0.803

4.3 Water Band Index across spectrum (WBIxxx)

WBIxxx tests the effect of variation in the strength of light absorption by water across the spectrum. Figure 4.8 illustrates the coefficient of determination between WBIxxx and available canopy biophysical variables in the FieldSpec measurements in Milingerwaard in 2004 and 2005 and the Korenburgerveen in 2008. Table 4.11 provides an overview of the maximum values in terms of R^2 with respect to all tested combinations of WBI in Eq. (4).

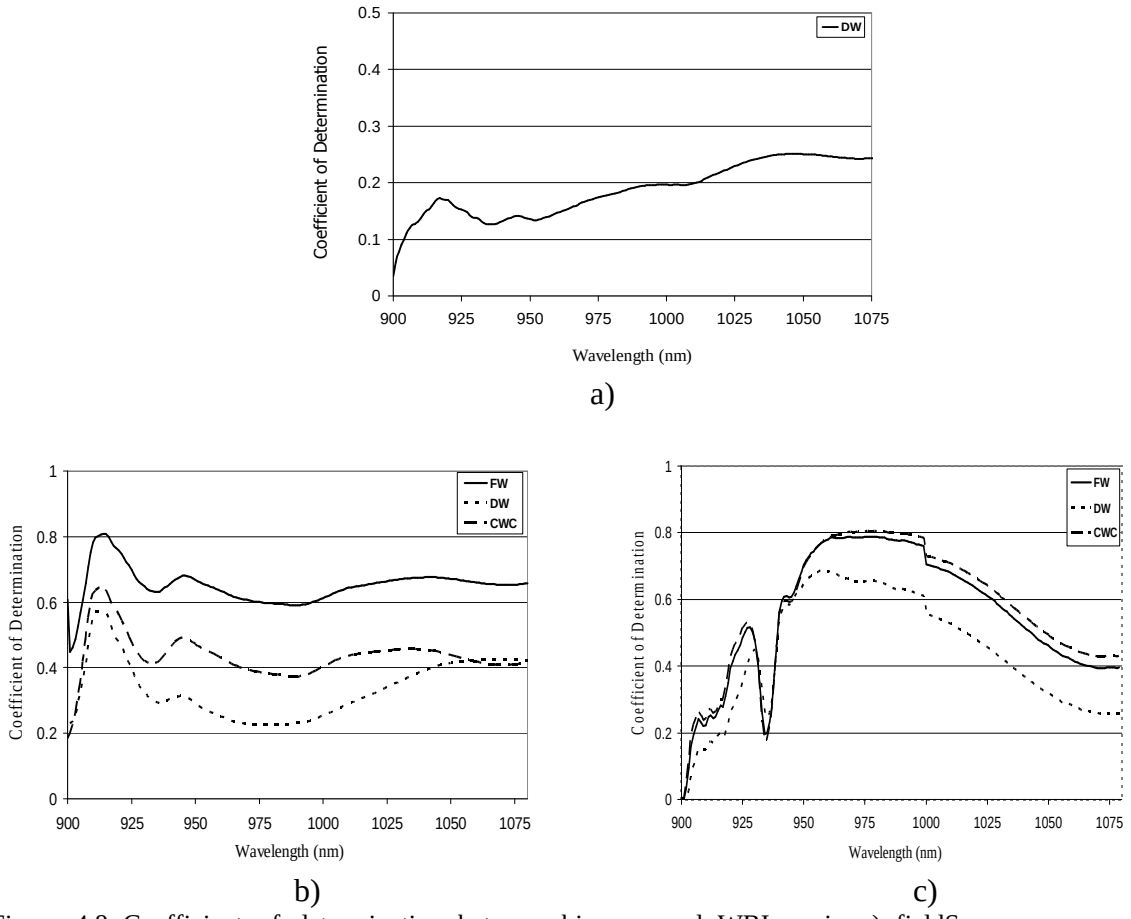

Figure 4.8 Coefficient of determination between biomass and WBIxxx in a) fieldSpec measurements in Milingerwaard in 2004 b) FieldSpec measurements in Millingerwaard in 2005 c) FieldSpec measurements in Korenburgerveen in 2008.

Table 4.11 Maximum Correlation coefficient of biomass and WBIxxx in three FieldSpec measurements

Data set in:	Biomass	Max R2(WBI, biomass)	Absorption feature
2004 (FieldSpec.)	DW	0.250	1048
2005 (FieldSpec.)	FW	**0.654**	914
	DW	0.572	914
	CWC	**0.649**	915
2008 (FieldSpec.)	FW	**0.789**	977
	DW	**0.686**	958
	CWC	**0.804**	977

4.4 Normalized difference water index

Table 4.12 shows the correlation coefficient and coefficient of determination between NDWI and biophysical variables in each dataset. Both datasets in 2004 show that there is not a statistically significant relationship between NDWI and DW with α 0.05 and 14 degrees of freedom in the FieldSpec data set and 15 degrees of freedom in the HyMap dataset. Results in 2005 show that the relationship between NDWI and both FW and CWC are significant with α 0.05 and 10 degrees of freedom. For the 2008 FieldSpec data, the correlation coefficient between NDWI and these three biophysical variables are statistically significant with α 0.05 and 37 degrees of freedom.

Table 4.12 Coefficient of Correlation between biomass and NDWI in each dataset.

Data set in:	df	p-value	Biomass	r(NDWI , biomass)	R2(NDWI , biomass)
2004 (FieldSpec.)	14	0.497	DW	0.494	0.245
(HyMap-1pixel)	15	0.482	DW	0.379	0.144
(HyMap-3*3pixels)				0.431	0.186
2005 (FieldSpec.)	10	0.576	FW	**0.590**	0.348
			DW	0.503	0.253
			CWC	**0.601**	0.361
2008 (FieldSpec.)	37	0.325	FW	**0.737**	0.543
			DW	**0.692**	0.478
			CWC	**0.738**	0.544

4.5 First derivative of spectra

Figure 4.9 illustrates the R2 between the first derivative and biophysical variables (FW, DW and CWC) in different data sets. In order to facilitate interpreting the wavelength positions in this figure, an example of one spectrum is added for illustration. This figure clearly shows that correlations depend on the spectral position. Region A in Figure 4.9 relates to the left slope of the absorption feature at about 970 nm. Region B relates to the right slope. Region C refers to the left slope of the absorption feature at about 1200 nm. Region D refers to the right slope of the later absorption feature. In general figure 4.9 shows that for many spectral positions beyond 900 nm the relationship between the first derivative and CWC, FW and DW are statistically significant at α 0.05. Figure 4.9a illustrates the relationship between DW and first derivative of spectra in the FieldSpec of Millingerwaard in 2004. The most significant coefficient of determination of 0.510 is found in region C at 1193.5 (meaning the difference between 1193 nm and 1194 nm). Figure 4.9b that refers to the HyMap considering one pixel for each sample plot. The most significant coefficient of determination (R2) of 0.451 is found in region B at 1000.6 nm. The most significant coefficient of determination of 0.628 is found in region D in figure 4.9c, which shows the relationship between first derivative of spectra in the HyMap image considering 3 by 3 pixels and DW. Figure 4.9d refers to the FieldSpec of Millingerwaard in 2005. It shows that the relationship between the first derivative and both FW and DW is statistically significant in all regions, whereas for CWC in region C it is only significant with a coefficient of determination of 0.446 at 1163.5 nm. Figure 4.9e illustrates that the relationship between the first derivatives of FieldSpec measurements of the Korenburgerveen and all three biophysical variables are statistically significant in each region. The most significant coefficient of determination between first derivatives and CWC of 0.408, which is found in region A at 966.5 nm.

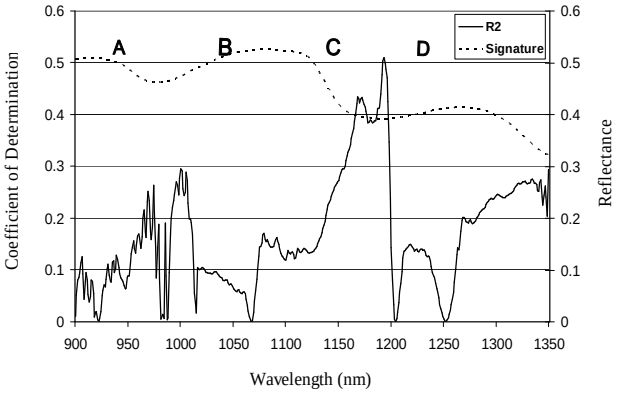

a)

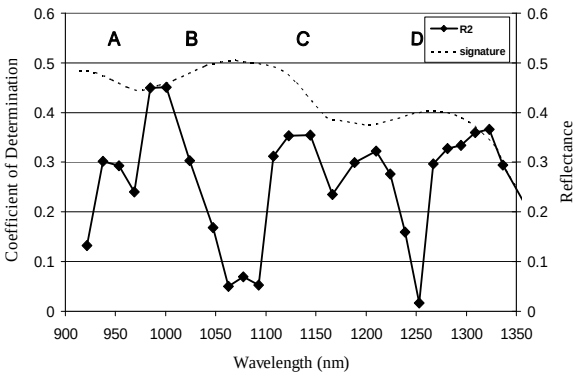

b)

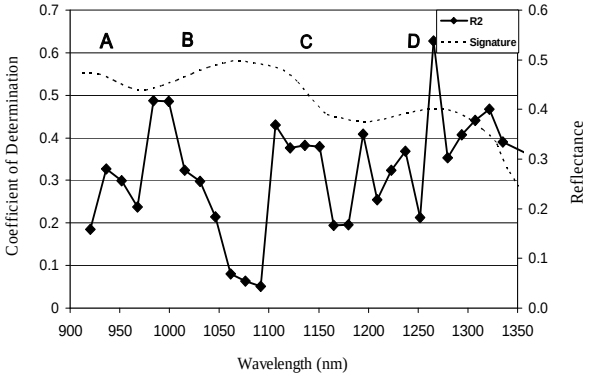

c)

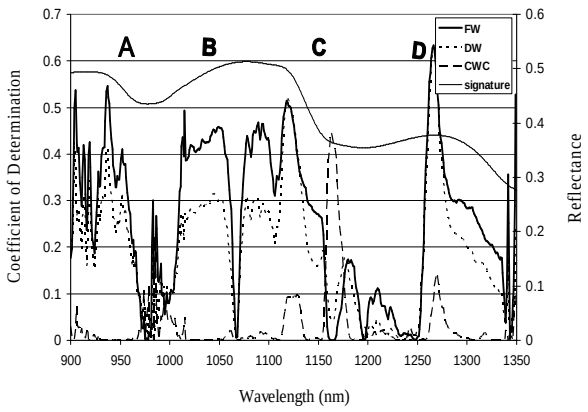

d)

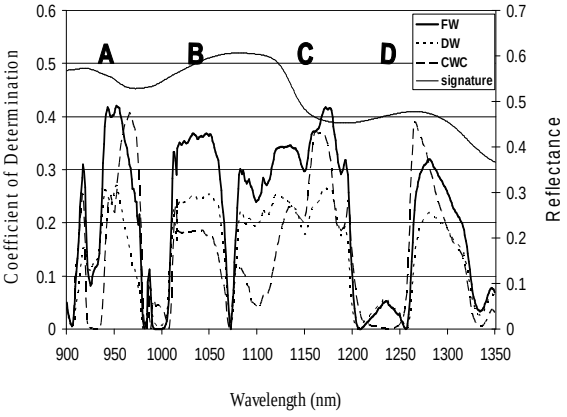

e)

Figure 4.9 Coefficient of determination between canopy biophysical variables and first derivative of canopy reflectance. a) FieldSpec derivatives with DW at the Millingerwaard test site in 2004. b) HyMap derivative with DW at the Millingerwaard test site (1pixel) in 2004. c) HyMap derivative with DW at the Millingerwaard test site (3*3pixels) in 2004. d) FieldSpec derivative with FW, DW and CWC at the Millingerwaard test site in 2005. e) FieldSpec derivative with FW, DW and CWC at the Korenburgerveen site in 2008.

5 DISCUSSION

In the first part of this thesis the continuum removal technique was applied to different intervals around the water absorption features at 970 nm and 1200 nm for estimating canopy water content, fresh weight and dry weight . Analyzing three datasets indicated different results. Test site 1 (FieldSpec measurements of Millingerwaard in 2004) shows that when a narrower interval is applied to the continuum removal technique the correlation between DW and indices based on the continuum removal technique is higher. Test site 2 (FieldSpec measurements of Millingerwaard in 2005) shows that while the interval is going to be narrower the correlation between canopy water content and MBD and AUC based on the continuum removal technique around water absorption feature will decrease (figure 4.2, 4.3 and 4.4). Test site 3 (Korenburgerveen in 2008) shows the constant coefficient of correlation between canopy water content and indices over several intervals. As shown data sets in Millingerwaard in 2004 and 2005 (figure 5.1a and 5.1b) have normal distribution. Figure 5.1b also shows that dry weight of sample plots was distributed in different ranges between minimum and maximum value. Whereas figure 5.1a shows that most of sample plots are located around the mean value for dry weight. Figure 5.1c shows that data set in the Korenburgerveen has skewed to the right. Thus, how to select the sample plots cause the difference in our results.

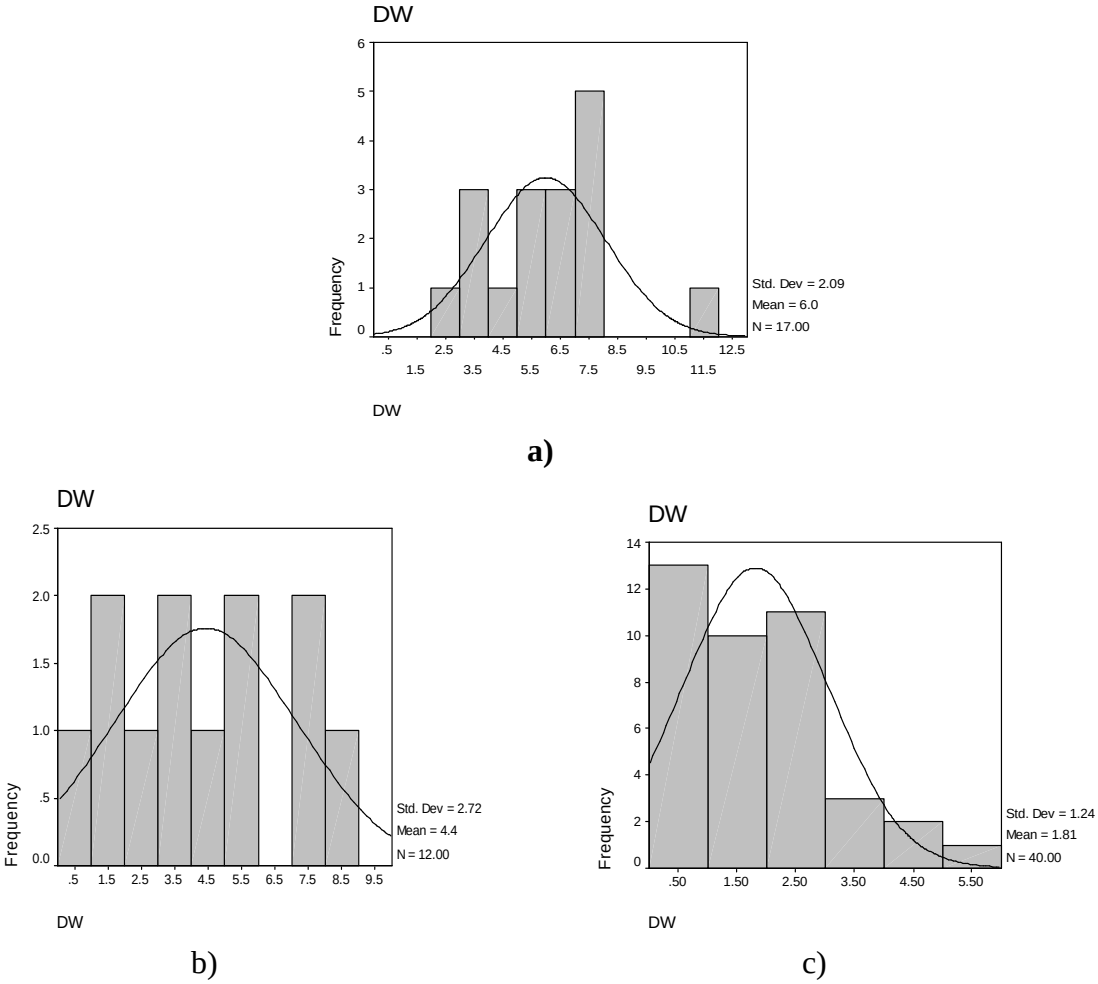

Figure 5.1 Frequency of DW in three data sets:

a) FieldSpec measurements of Millingerwaard in 2004

b) FieldSpec measurements of Millingerwaard in 2005

c) FieldSpec measurements of Korenburgerveen in 2008

Another difference between the datasets in the Millingerwaard and Korenburgerveen is related to the values of the correlation coefficient between biophysical variables (CWC, FW and DW) and indices. FieldSpec measurements of Korenburgerveen in 2008 show much higher correlation than FieldSpec measurements of Millingerwaard in 2004 and 2005. To investigate why there is such a difference between these two data sets looking at vegetation indices such as NDVI can be useful. Figure 5.2 illustrates the scatter plot for fresh weight as a function of NDVI in FieldSpec measurements in Millingerwaard in 2005 and Korenburgerveen in 2008. Figure 5.2a shows that most of the sample plots have the same value of NDVI (around 0.9) in Milingerwaard. Figure 5.2b illustrates a broader range for NDVI in Korenburgerven than for Millingerwaard. Since NDVI is directly related to the photosynthetic capacity and hence energy absorption of plant canopies, the difference in correlation can be affected by species type.
Also it was already mentioned that the Korenburgerveen site is a homogeneous and Millingerwaard is a heterogeneous area, therefore the probability of having several species types in one sample plot in Milingerwaard is much larger than in Korenburgerveen. So, this variety in species types can cause less correlation between biophysical variables (CWC, FW and DW) and indices.

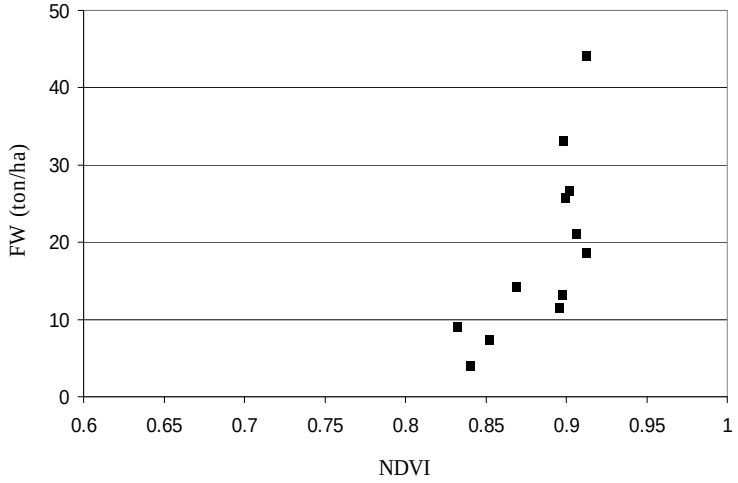

a)

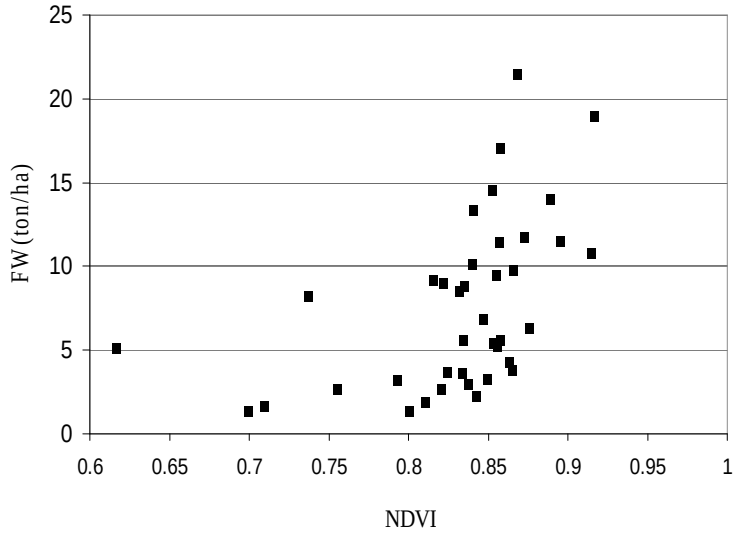

Figure 5.2 Fresh weights as a function of NDVI in a) Millingerwaard in 2005, b) Korenburgerveen in 2008

Results show that there is not a statistically significant difference between the coefficient of determination between biophysical variables (FW, DW and CWC) and the continuum removal indices over different intervals.
In the second part of this thesis the continuum removal technique has been applied for the HyMap image to find out which index has the highest relationship with DW (just DW was available). Results show that in the water absorption feature at 970 nm MBD and AUC for broader intervals and MBD/AUC and AUC/MBD for narrower intervals have a higher coefficient of correlation with DW. But at the water absorption features at 1200 nm both intervals show nearly the same coefficient of correlation. By looking at the table in appendix 9 we discovered that the correlation between DW and continuum removal indicators is not statistically significantly different from there being no correlation. Whereas the objective of this part was to investigate the effect of which index based on the continuum removal technique is better for estimation of DW. In each step the effect of two indices with α of 0.05 was compared (see examples 1 and 2 in appendix 10). Result shows there is not a statistically significant difference between indices based on the continuum removal technique.
Finally, in last part of this thesis a comparison is made between indices mentioned in the literature review on estimation of CWC for test site 2 and 3 and estimation of DW for test site 1. Table 5.1 provides an overview of all results in terms of R^2 values.

Table 5.1 Rresults for the indices tested in estimating canopy water content (site2 and 3) or just dry weight (site1) as shown by the coefficient of determination (R^2).

	Site1 FieldSpec	**Site1 HyMap (1pixel)**	**Site1 HyMap (3*3pixels)**	**Site2 FieldSpec**	**Site3 FieldSpec**
Best derivative	0.51@1193.5	0.628@1265.75	0.487@983.6	0.446@1163.5	0.408@966.5
WBI	0.165	0.161	0.179	0.397	0.803
NDWI	0.245	0.144	0.186	0.361	0.544
970 nm feature					
MBD	0.048	0.176	0.197	0.312	0.843
AUC	0.041	0.153	0.162	0.373	0.815
MBD/AUC	0.000	0.102	0.007	0.529	0.088
AUC/MBD	0.000	0.009	0.100	0.540	0.091
1200nm feature					
MBD	0.067	0.102	0.085	0.295	0.734
AUC	0.066	0.091	0.075	0.309	0.723
MBD/AUC	0.002	0.126	0.126	0.234	0.141
AUC/MBD	0.002	0.127	0.128	0.236	0.147

Site1: FieldSpec measurements in Millingerwaard in 2004
Site2: FieldSpec measurements in Millingerwaard in 2005
Site3: FieldSpec measurements in Korenburgerveen in 2008

The WBI performed better than the NDWI in the estimation of the canopy water content in terms of significance. Results for the continuum removal methods (applied to either of the water absorption features) were clearly worse for the heterogenous area (site 1 and 2) and clearly better for the homogeneous area (site 3). Also the scatter plot of canopy water content as a function of MBD in Figure 5.3 shows that canopy water content is highly correlated to the MBD at water absorption feature 970 nm in a homogeneous area (Korenburgerveen).

Whereas there is not a clear relationship between canopy water content and the maximum band depth in a heterogeneous area (Millingerwaard).
The MBD and AUC for the water absorption feature at 1200 nm performed worse than for the water absorption feature at 970 nm, whereas MBD/AUC and AUC/MBD for the water absorption feature at 1200 nm performed better than at 970 nm on the estimation of canopy water content in terms of significance.

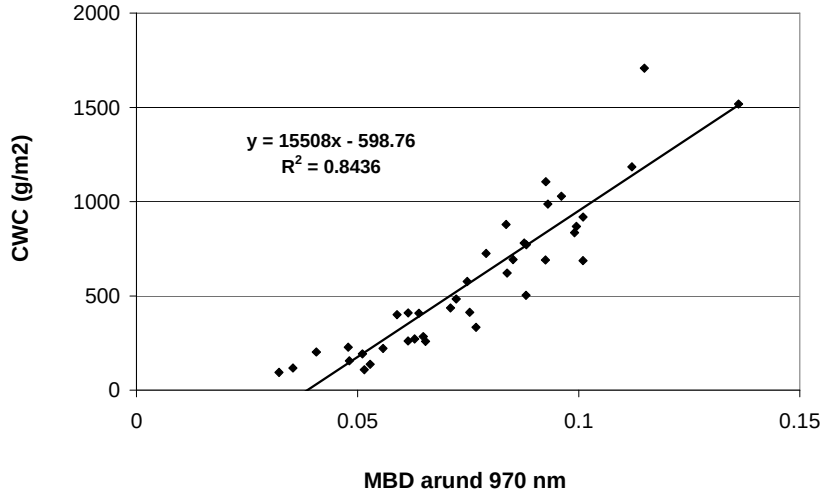

a)

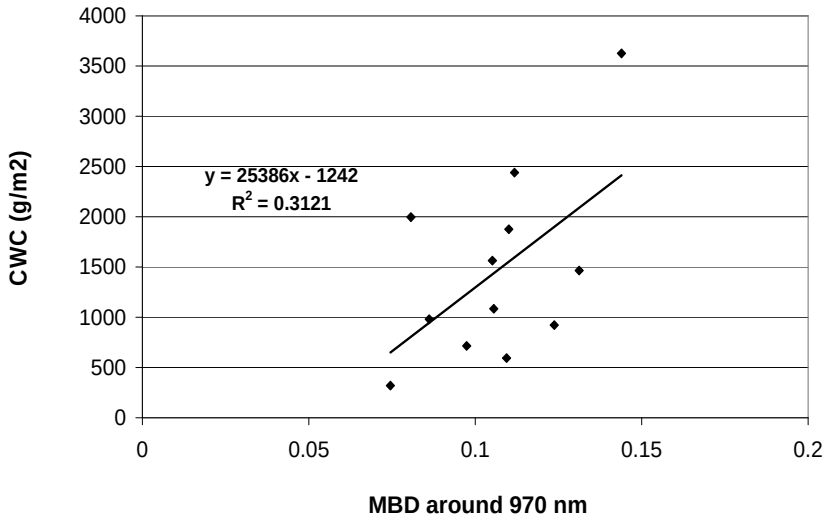

b)

Figure 5.3 Canopy water content as a function of MBD at water absorption feature 970 nm.

a) Korenburgerveen in 2008

b) Millingerwaard in 2005

6 CONCLUSION AND RECOMMENDATION

6.1 Conclusion

The objective of this thesis was to apply the continuum removal technique to the water absorption features in the NIR region to estimate canopy water content and biomass. Objective was also to compare the results of the continuum removal method to WI, NDWI and first derivative of spectra.
Result presented in this report show that for the FieldSpec measurements, indices based on the continuum removal method (MBD, AUC, MBD/AUC and AUC/MBD) have higher correlation with canopy biophysical variables for broader intervals at the water absorption features 970 nm and 1200 nm. Results yielded that MBD and AUC have clearly a stronger correlation with biophysical variables than other continuum removal indicators at both water absorption features in the NIR region in a homogenous area. For a heterogeneous area MBD/AUC and AUC/MBD at 970 nm and MBD and AUC at 1200 nm have higher correlation with canopy biophysical variables.

Results for the HyMap data set (both considering one pixel and 3 by 3 pixels for each plot) yielded that the MBD and AUC for broader intervals and MBD/AUC and AUC/MBD for narrower intervals have a higher correlation with canopy biophysical variables at the water absorption features 970 nm and shows that canopy biophysical variables have the same correlation with continuum removal indicators for broader and narrower intervals at the water absorption feature 1200 nm. For both water absorption features of HyMap, MBD/AUC and AUC/MBD have the best effect on estimating dry weight.

The last part of this thesis focused on the effect of different indices on the estimation of canopy biophysical variables. Result showed that the first derivative of the spectra is much better than continuum removal indices and clearly better than WBI and NDWI in the estimation of canopy biophysical variables in a heterogeneous area. Whereas in a homogeneous area (site 3) continuum removal indices (only MBD and AUC) yielded stronger effects on estimation of canopy biophysical variables and the first derivative yielded the worst results.
Derivatives provide better results for heterogeneous area and MBD and AUC provide better results in this study than reflectance or indices as used in literature (Sims and Gamon, 2003; Clevers & Kooistra, 2006).

An advantage of derivative spectra is their insensitivity to variations in soil background and atmospheric effects (Clevers et al., 2001). As a result, derivative spectra also will be insensitive to the presence of yellow, dry vegetation and litter, making them attractive as estimator for canopy water content.

6.2 Recommendations

Further analyzing is required to focus on the dependency of the result on plant functional type. To get a better conclusion for the first part of this thesis it would be better to have different datasets of FieldSpec measurements for each type of area (homogonous and heterogeneous) with the same size and same numbers of sample plots and the same sampling method.

The maximum band depth and the area under the curve have the higher correlation with canopy water content in homogeneous area than in heterogeneous area, so we wish to test on more than these two test sites to be sure about this result.

Reference:

Ceccato P. N., Gobron S., Flasse B., Pinty, & S. Tarantola, 2002, "Designing a spectral index to estimate vegetation water content from remote sensing data" *Remote sensing of environment* **82** 188-197.

Champagne, C., Pattey, E., Bannari, A., and Stratchan, I.B., 2001. "Mapping Crop Water Status: Issues of Scale in the Detection of Crop Water Stress Using Hyperspectral Indices". *Proceedings of the 8th International Symposium on Physical Measurements and Signatures in Remote Sensing, Aussois, France,* 79-84.

Chuvieco E., Cocero D., Riono D., Martin P., Martinez J., Perez F., et al., 2004, "Combining NDVI and surface temperature for the estimation of live fuel moisture content in forest fire danger rating" *Remote sensing of environment* **92** 322-331

Clark R. N. & Roush T. L., 1984, "Reflectance spectroscopy: quantitative analysis techniques for remote sensing applications" *Journal of geophysical research* **89** 6329-6340.

Clevers, J.G.P.W., de Jong, S.M., Epema, G.F., van der Meer, F., Bakker, W.H., Skidmore, A.K., Addink, E.A., 2001. "MERIS and the red-edge position". *International Journal of Applied Earth Observation and Geoinformation* **3 (4)**, 313–320

Clevers, J.G.P.W., Kooistra L., 2006. "Using spectral information at the NIR water absorption features to estimate canopy water content and biomass". *ISPRS mid-term symposium remote sensing: from pixels to processes, 8-11 May, Enschede, The Netherlands*, pp. 6.

Curran, P. J., 1989. "Remote sensing of foliar chemistry". *Remote Sensing of Environment*, **30** 271-278.

Danson F. M., Steven M. D., Malthus T. J., & Clark J. A., 1992, "High-spectral resolution data for determining leaf water content" *International journal of remote sensing* **13** 461-470.

ESA, 2006. "The Changing Earth". *SP-1304*, 83 pp.

Gao B. C., Goetz A. F., 1995, "Retrieval of equivalent water thickness and information related to biochemical components of vegetation canopies from AVIRIS data". *Remote Sensing of Environment* **52** 155–162.

Gao B.C., 1996, "NDWI - A normalized difference water index for remote sensing of vegetation liquid water from space". *Remote sensing of environment* **58** 257-266.

Hardisky M.A., Klemas V., and Smart R.M., 1983. "The Influences of Soil Salinity, Growth Form, and Leaf Moisture on the Spectral Reflectance of Spartina Alterniflora Canopies". Photogrammetric Engineering and Remote Sensing 49 77-83.

Hunt Jr. E.R., & Rock, B.N., 1989. "Detection of Changes in Leaf Water Content Using Near-And Middle-Infrared Reflectances". *Remote Sensing of Environment* **30** 43-54.

Iqbal, M., 1983. "An introduction to solar radiation". *Academic Press, Ontario*, 390 pp.

Jackson T.L., Chen D., Cosh M.,. Anderson F. Li, M, Walthall C., Doriaswamy P., and Hunt E.R., 2004. "Vegetation Water Content Mapping Using Landsat Data Derived Normalized Difference Water Index for Corn and Soybeans". *Remote Sensing of Environment* **92** 475-482.

Keller, P.A., 2001. "Imaging spectroscopy of lake water quality parameters". *Ph.D. Thesis. Remote Sensing Series 36, RSL, University of Zurich*, 161.

Kokaly R. F., Clark R. N. 1999, "Spectroscopic determination of leaf biochemistry using band-depth analysis of absorption features and stepwise multiple linear regression" *Remote sensing of environment* **67** 267-287.

Kooistra, L., Suarez Barranco M.D., Van Dobben H., E Schaepman M.E., 2006. "Regional scale monitoring of vegetation biomass in river floodplains using imaging spectroscopy and ecological modeling". *Proceedings IGARRS '06 Symposium, Denver, Colorado,* 124-127.

Kooistra, L., Sterkx, S., , Liras laita, E., Mengesha, T., Verbeiren, B., Batelaan, O., Vandobben, H., Schaepman, M.E., Schaepman-Strub, G., And Struiver, J. 2005 *HyEco04: An airborne imaging spectroscopy campaign in the floodplain the Millingerwaard, the Netherlands. CGI-report, Wageningen UR, Wageningen.*

Palmer k.f., Williams D., 1974 "optical properties of water in the near infrared". *Optical Society* **64** 1107-1110.

Penuelas J., Filella I., Biel C., Serrano L., & Save R., 1993, "The reflectance at the 950-970 nm region as an indicator of plant water status" *International journal of remote sensing* **14** 1887-1905.

Penuelas J., Pinol J., Ogaya R., & Filella I. 1997, "Estimation of plant water concentration by the reflectance Water Index WI (R900/R970)" *International journal of remote sensing* **18** 2869-2875.

Richter, R. & Schlapfer, D. 2002, "Geo-atmospheric processing of airborne imaging spectrometry data. Part 2: atmospheric/topographic correction". *International Journal of Remote Sensing,* **23** 2631-2649.

Riano, D., Vaughan, P., Zarco-Tejada, E., & Ustin, P. J., 2005. "Estimation of fuel moisture content by inversion of radiative transfer models to simulate equivalent water thickness and dry matter content. Analysis at leaf and canopy level". *IEEE Transactions on Geoscience and Remote Sensing,* **43** 819−826.

Rollin, E. M., and Milton, E. J., 1998. "Processing of high spectral resolution reflectance data for the retrival of vanopy water content information". *Remote Sensing of Environment,* **65** 86-92

Rouse, J.W., Haas, R.H., Schell, J.A. and Deering, D.W., 1973. "Monitoring Vegetation Systems in the Great Plains with ERTS". *Third ERTS Symposium, NASA SP-351* I 309-317.

Running, S.W. & Coughlan, J.C. 1988. "A general-model of forest ecosystem processes for regional applications .1. Hydrologic balance, canopy gas-exchange and primary production Processes". Ecological Modelling, 42 125- 154.

Schaepman-Strub, G, Schaepman, M.E., Painter, T.H., Dangel S. & Martonchik, J.V., 2006. "Reflectance quantities in optical remote sensing-definitions and case studies". *Remote Sensing of Environment*, **103** 27-42.

Schaepman, M.E., Wamelink, G.W.W., Van Dobben, H.F., Gloor, M., Schaepman-Strub, G., Kooistra, L., Clevers, J.G.P.W., Schmidt, A., Berendse, F., 2007. "River floodplain vegetation scenario development using imaging spectroscopy derived products as input variables in a dynamic vegetation model". *Photogrammetric Engineering and Remote Sensing* **73** 1179–1188.

Schlapfer D., Richter R., 2002. "Geo-atmospheric processing of airborne imaging spectrometry data. Part 1: parametric orthorectification". International Journal of Remote Sensing 23, 2609–2630.

Sellers, P.J., 1985. "Canopy Reflectance, Photosynthesis and Transpiration". *International Journal of Remote Sensing* **6** 1335-1372.

Serrano L., Ustin S. L., Roberts D. A., Gamon J. A., & Penuelas J., 2000. "Deriving water content of chaparral vegetation from AVIRIS data". Remote Sensing of Environment, 74 570– 581.

Sims D.A., & Gamon, J.A. 2003, " Estimation of vegetation water content and photosynthetic tissue area from spectral reflectance: a comparison of indices based on liquid water and chlorophyll absorption features" *Remote Sensing of Environment* 84, 526–537

Tian Q., Tong Q., Pu R., Guo, X., & Zhao C., 2001. "Spectroscopic determinations of wheat water status using 1650 – 1850 nm spectral absorption features". International Journal of Remote Sensing, 22 2329– 2338.

Tucker, C.J., 1979. "Red and Photographic Infrared Linear Combinations for Monitoring Vegetation". *Remote Sensing of the Environment* **8** 127-150.

Ustin S.L., Roberts D.A., Pinzon J., Jacquemoud S., Gardner M., Scheer G., 1998, "Estimating canopy water content of chaparral shrubs using optical methods" *Remote sensing of environment* **65** 280-291

Ustin, S.L., Darling, D., Kefauver, S., Greenberg, J., Cheng, Y.B., &Whiting, M. L. 2004a. "Remotely sensed estimates of crop water demand". *S.P.I.E. the international symposium on optical science and technology. 49th annual meeting, Denver, CO, 2–6 August.*

Ustin, S. L., Jacquemoud, S., Zarco-Tejada, P. J., and Asner, G., 2004b. "Remote Sensing of Environmental Processes, State of the Science and New Directions. in Manual of Remote Sensing Vol. 4. Remote Sensing for Natural Resource Management and Environmental Monitoring. ASPRS. John Wiley and Sons, New York 768p. +cd. ASPRS. John Wiley and Sons, New York, pages 679-730

Zarco-Tejada, P.J., Rueda, C.A., & Ustin, S. L. 2003. "Water content estimation in vegetation with MODIS reflectance data and model inversion methods". *Remote Sensing of Environment,* **85** 109−124.

Appendix 1- Vegetation description

Vegetation descriptions were made according to the method of Braun-Blanquet(1951). Abundance per species was estimated optically as percentage soil covered by living biomass in vertical projection, and scored in a nine-point scale. All bryophytes and lichens, and also vascular species that were not readily recognisable in the field, were collected for later identification. Taraxacum species were taken together as T. vulgare, and Rubus species were taken together as R. fruticosus, except R. caesius. No subspecific taxa were used. Nomenclature follows van der Meijden et al. (1990), Touw & Rubers (1989), and Brand et al. (1988) for vascular species, mosses and lichens, respectively. No distinction in layers (e.g. by using pseudo-species) was made. Syntaxonomic nomenclature follows Schaminée et al. (1995, 1996, and 1998). In total, 79 species were found in the plots in the Millingerwaard. The number of occurrences in the total of 20 plots is listed below.

Code	Number of occurrences	Full name
Achilmil	5	Achillea millefolium L.
Agrossto	5	Agrostis stolonifera L.
Arctilap	9	Arctium lappa L.
Arrheela	2	Arrhenatherum elatius (L.) J.& C.Presl
Atrippat	2	Atriplex patula L.
Brassnig	7	Brassica nigra (L.) Koch
Bromuine	3	Bromus inermis Leysser
Calamepi	10	Calamagrostis epigejos (L.) Roth
Calyssep	2	Calystegia sepium (L.) R.Br.
Cardunut	2	Carduus nutans L.
Carexhir	6	Carex hirta L.
Cerasfon	3	Cerastium fontanum Baumgarten
Cirsiarv	15	Cirsium arvense (L.) Scopoli
Cirsivul	2	Cirsium vulgare (Savi) Tenore
Cratamon	1	Crataegus monogyna Jacquin
Cynoddac	2	Cynodon dactylon (L.) Persoon
Dactyglo	5	Dactylis glomerata L.
Dipsaful	1	Dipsacus fullonum L.
Elymurep	9	Elymus repens (L.) Gould
Epilohir	3	Epilobium hirsutum L.
Epilotet	3	Epilobium tetragonum L.
Equisarv	1	Equisetum arvense L.
Erigecan	5	Erigeron canadensis L.
Eryngcam	6	Eryngium campestre L.
Euphocyp	1	Euphorbia cyparissias L.
Euphoesu	4	Euphorbia esula L.
Festurub	7	Festuca rubra L.

Galeotet	2	Galeopsis tetrahit L.
Galiuapa	4	Galium aparine L.
Galiumol	2	Galium mollugo L.
Geranpus	1	Geranium pusillum L.
Glechhed	10	Glechoma hederacea L.
Hernigla	5	Herniaria glabra L.
Hyperper	2	Hypericum perforatum L.
Iris pse	1	Iris pseudacorus L.
Linarvul	1	Linaria vulgaris Miller
Loliuper	2	Lolium perenne L.
Lycopeur	2	Lycopus europaeus L.
Lythrsal	2	Lythrum salicaria L.
Matrimar	3	Matricaria maritima L.
Mediclup	1	Medicago lupulina L.
Melilalt	2	Melilotus altissima Thuillier
Menthaqu	2	Mentha aquatica L.
Myosoarv	1	Myosotis arvensis (L.) Hill
Myosol-c	1	Myosotis laxa (subsp. cespitosa) (Schultz) Nordh.
Odontver	3	Odontites vernus (Bellardi) Dumortier
Oenotbie	2	Oenothera biennis L.
Pastisat	1	Pastinaca sativa L.
Phalaaru	1	Phalaris arundinacea L.
Phleupra	2	Phleum pratense L.
Plantlan	2	Plantago lanceolata L.
Plantmaj	1	Plantago major L.
Poa ann	2	Poa annua L.
Poa pra	3	Poa pratensis L.
Poa tri	11	Poa trivialis L.
Polynper	3	Polygonum persicaria L.
Potenans	5	Potentilla anserina L.
Potenrep	11	Potentilla reptans L.
Prunevul	1	Prunella vulgaris L.
Ranunrep	3	Ranunculus repens L.
Roripaus	1	Rorippa austriaca (Crantz) Besser
Rubuscae	8	Rubus caesius L.
Rumexace	3	Rumex acetosa L.
Rumexcri	2	Rumex crispus L.
Rumexobt	1	Rumex obtusifolius L.

Saponoff	2	Saponaria officinalis L.
Seneceru	1	Senecio erucifolius L.
Senecina	5	Senecio inaequidens DC.
Senecjac	4	Senecio jacobaea L.
Solandul	1	Solanum dulcamara L.
Solidcan	3	Solidago canadensis L.
Stellaqu	2	Stellaria aquatica (L.) Scopoli
Tanacvul	2	Tanacetum vulgare L.
Taraxoff	4	Taraxacum officinale s.s. Wiggers
Trifofra	1	Trifolium fragiferum L.
Triforep	5	Trifolium repens L.
Urticdio	10	Urtica dioica L.
Verbanig	2	Verbascum nigrum L.

Refrence: L. Kooistra, S. Sterkx, E. Liras Laita, T. Mengesha, B. Verbeiren, O. Batelaan, H. van Dobben, M. Schaepman, G. Schaepman&Strub and J. Stuiver "HyEco’04: an airborne imaging spectroscopy campaign in the floodplain Millingerwaard, the Netherlands.Quality assessment of field and airborne data" CGI Report 2005&07.

Appendix 2- Measured weight for the individual samples in Millingerwaard in 2005.

	Plot	VALERI	Fresh Weight	Dry Weight
PFT	Nr.	Location	g/m2	g/m2
shrub	1	A	4737.56	923.84
Shrub	1	C	3525.2	433.08
shrub	1	E	4999.48	1027.24
herb	2	A	555.68	113.6
herb	2	C	1613.88	380.24
herb	2	E	2106	528.12
herb	3	A	497.88	1011.6
herb	3	C	679	194.84
herb	3	E	1561.4	296.44
herb	4	A	2114.48	456.6
herb	4	C	957.92	196.88
herb	4	E	2538.88	562.84
shrub	5	A	2050.56	540.88
Shrub	5	C	2312.92	684.16
shrub	5	E	3661.72	1170.96
herb	6	A	881.76	141
herb	6	C	635.12	133.56
herb	6	E	682.16	143
herb	7	A	2687.2	680.4
herb	7	C	1767.12	589.84
herb	7	E	1866.28	357.84
herb	8	A	1518.84	487.36
herb	8	C	1331.72	286.48
herb	8	E	1105.84	242.4
shrub	9	A	4570.12	1155.44
Shrub	9	C	4107.4	1155.72
shrub	9	E	1247.4	333.48
shrub	10	A	2747.88	485.32
Shrub	10	C	1998.04	641.8
shrub	10	E	2967.2	597.4
herb	12	A	429.12	84.04
herb	12	C	271	31.6
herb	12	E	489.84	115.64
herb	14	A	803.08	151.04
herb	14	C	1505.12	314.24

Appendix 3- Measured weight for the individual plots in the Millingerwaard in 2005.

Plot Nr.	fresh weight g/m2	dry weight g/m2	water weight g/m2
1	4420.75	794.72	3626.03
2	1425.19	340.65	1084.53
3	912.76	197.63	715.13
4	1870.43	405.44	1464.99
5	2675.07	798.67	1876.40
6	733.01	139.19	593.83
7	2106.87	542.69	1564.17
8	1318.80	338.75	980.05
9	3308.31	868.21	2440.09
10	2571.04	574.84	1996.20
12	396.65	77.09	319.56
14	1154.10	232.64	921.46

Appendix 4- Measured dry weight for the individual plots in the Millingerwaard in 2004.

Plot	dry weight
Nr.	g/m2
2	142.88
3	623.08
4	715.68
5	142.08
6	580.8
7	602.36
8	709.72
9	714.48
10	736.56
11	1164.64
12	741.24
13	127.32
14	572.44
15	395.96
16	368.24
17	646.08
18	241.88
19	489.64
20	508.52
21	258.68
22	371

Appendix 5- Measured weight for the individual samples in the Korenburgerveen in 2008.

Plot Nr.	VALERI Location	Fresh Weight g/m2	Dry Weight g/m2
1	A	760	177
1	C	1496	298
1	E	1200	226
2	A	1848	425
2	C	880	215
2	E	1288	289
3	A	920	205
3	C	904	179
3	E	840	201
4	A	304	75
4	C	640	136
4	E	344	76
5	A	1008	235
5	C	1136	251
5	E	1104	255
6	A	760	164
6	C	680	146
6	E	464	142
7	A	880	234
7	C	2176	402
7	E	2632	499
8	A	1616	343
8	C	3192	635
8	E	1640	340
9	A	792	169
9	C	848	226
9	E	1400	302
10	A	808	211
10	C	424	119
10	E	816	208
11	A	248	53
11	C	288	54
11	E	544	119
12	A	944	208
12	C	896	182
12	E	1104	238
13	A	2352	900
13	C	1008	249
13	E	1008	257
14	A	424	88
14	C	656	137
14	E	456	86

Plot Nr.	VALERI Location	Fresh Weight g/m2	Dry Weight g/m2
15	A	672	134
15	C	664	149
15	E	344	89
16	A	1544	344
16	C	1136	277
16	E	760	182
17	A	1624	419
17	C	848	221
17	E	1056	282
18	A	136	32
18	C	192	43
18	E	96	23
19	A	1224	240
19	C	1912	426
19	E	1072	226
20	A	656	157
20	C	880	215
20	E	1304	291
21	A	268	89
21	C	280	89
21	E	144	46
22	A	336	93
22	C	320	82
22	E	248	63
23	A	680	184
23	C	296	94
23	E	120	41
24	A	512	166
24	C	416	114
24	E	232	65
25	A	32	13
25	C	24	8
25	E	16	5
26	A	216	63
26	C	120	33
26	E	64	21
27	A	152	40
27	C	136	50
27	E	216	60
28	A	328	92
28	C	192	79
28	E	288	58

Plot Nr.	VALERI Location	Fresh Weight g/m2	Dry Weight g/m2
29	A	384	98
29	C	616	172
29	E	624	153
30	A	416	87
30	C	360	66
30	E	208	47
31	A	168	39
31	C	704	163
31	E	704	136
32	A	1208	355
32	C	2960	951
32	E	936	243
33	A	288	72
33	C	232	59
33	E	280	61
34	A	1448	336
34	C	1024	236
34	E	240	68
35	A	224	70
35	C	296	76
35	E	56	17
36	A	1016	251
36	C	1032	271
36	E	712	176
37	A	664	169
37	C	544	156
37	E	480	132
38	A	1780	481
38	C	584	161
38	E	200	58
39	A	392	95
39	C	368	122
39	E	208	66
40	A	600	166
40	C	712	216
40	E	1152	352

Appendix 6- Measured weight for the individual plots in the Korenburgerveen in 2008

Plot Nr.	fresh weight g/m2	dry weight g/m2	water weight g/m2
1	1152	233.56	918.44
2	1338.67	309.76	1028.91
3	888	195.07	692.93
4	429.33	95.83	333.51
5	1082.67	246.92	835.75
6	634.67	150.51	484.16
7	1896	378.32	1517.68
8	2149.33	439.57	1709.76
9	1013.33	232.56	780.77
10	682.67	179.25	503.41
11	360	75.48	284.52
12	981.33	209.36	771.97
13	1456	468.87	987.13
14	512	103.63	408.37
15	560	123.61	436.39
16	1146.67	267.63	879.04
17	1176	307.33	868.67
18	141.33	32.64	108.69
19	1402.67	297.01	1105.65
20	946.67	220.84	725.83
21	230.67	74.53	156.13
22	301.33	79.49	221.84
23	365.33	106.37	258.96
24	386.67	114.80	271.87
25	24	8.57	15.43
26	133.33	38.96	94.37
27	168	50.03	117.97
28	269.33	76.61	192.72
29	541.33	140.75	400.59
30	328	66.76	261.24
31	525.33	112.24	413.09
32	1701.33	516.47	1184.87
33	266.67	64.16	202.51
34	904	213.31	690.69
35	192	54.12	137.88
36	920	232.56	687.44
37	562.67	152.64	410.03
38	854.67	233.27	621.40
39	322.67	94.37	228.29
40	821.33	244.67	576.67

Appendix 7: HyMap Band Positions

Module	Module Band	HyMap Band	Center Wvl	Atmo. Corr. Wvl.	FWHM
VIS	1	1	445.00	442.00	8.10
VIS	2	2	454.70	451.70	13.60
VIS	3	3	469.30	466.30	16.50
VIS	4	4	485.20	482.20	15.60
VIS	5	5	500.10	497.10	15.60
VIS	6	6	515.00	512.00	15.40
VIS	7	7	530.70	527.70	16.40
VIS	8	8	546.30	543.30	15.90
VIS	9	9	561.40	558.40	15.20
VIS	10	10	576.30	573.30	15.30
VIS	11	11	591.50	588.50	15.50
631VIS	12	12	607.00	604.00	16.10
VIS	13	13	622.50	619.50	15.30
VIS	14	14	637.60	634.60	15.40
VIS	15	15	652.60	649.60	15.10
VIS	16	16	667.60	664.60	15.30
VIS	17	17	682.80	679.80	15.50
VIS	18	18	698.20	695.20	15.90
VIS	19	19	713.50	710.50	15.30
VIS	20	20	728.50	725.50	15.20
VIS	21	21	743.50	740.50	15.40
VIS	22	22	758.70	755.70	15.60
VIS	23	23	773.80	770.80	15.10
VIS	24	24	788.60	785.60	15.30
VIS	25	25	803.70	800.70	15.60
VIS	26	26	818.90	815.90	15.70
VIS	27	27	834.10	831.10	15.60
VIS	28	28	849.20	846.20	15.90
VIS	29	29	864.50	861.50	16.20
VIS	30	30	879.60	876.60	16.20
NIR	1	31	880.50	879.35	16.90
NIR	2	32	897.10	895.95	16.10
NIR	3	33	913.30	912.15	16.70
NIR	4	34	929.40	928.25	16.00
NIR	5	35	945.20	944.05	15.90
NIR	6	36	961.10	959.95	16.20
NIR	7	37	976.80	975.65	16.10
NIR	8	38	992.70	991.55	15.90
NIR	9	39	1008.50	1007.35	15.70
NIR	10	40	1024.10	1022.95	15.90

NIR	11	41	1039.60	1038.45	15.50
NIR	12	42	1055.00	1053.85	15.30
NIR	13	43	1070.10	1068.95	15.50
NIR	14	44	1085.20	1084.05	15.40
NIR	15	45	1100.30	1099.15	15.20
NIR	16	46	1115.10	1113.95	15.10
NIR	17	47	1130.00	1128.85	15.30
NIR	18	48	1144.70	1143.55	15.10
NIR	19	49	1159.20	1158.05	14.80
NIR	20	50	1173.80	1172.65	15.20
NIR	21	51	1188.50	1187.35	15.20
NIR	22	52	1202.80	1201.65	14.80
NIR	23	53	1217.00	1215.85	14.90
NIR	24	54	1231.40	1230.25	15.20
NIR	25	55	1245.80	1244.65	15.00
NIR	26	56	1259.90	1258.75	14.80
NIR	27	57	1273.90	1272.75	14.80
NIR	28	58	1288.00	1286.85	14.90
NIR	29	59	1301.90	1300.75	14.80
NIR	30	60	1315.90	1314.75	14.90
NIR	31	61	1329.90	1328.75	14.80
NIR	32	62	1343.30	1342.15	14.50
SWIR1	1	63	1403.90	1404.40	15.50
SWIR1	2	64	1418.40	1418.90	15.60
SWIR1	3	65	1432.50	1433.00	15.50
SWIR1	4	66	1446.80	1447.30	15.50
SWIR1	5	67	1460.80	1461.30	14.90
SWIR1	6	68	1474.70	1475.20	15.10
SWIR1	7	69	1488.60	1489.10	15.10
SWIR1	8	70	1502.40	1502.90	14.80
SWIR1	9	71	1515.90	1516.40	14.70
SWIR1	10	72	1529.10	1529.60	14.90
SWIR1	11	73	1542.70	1543.20	15.20
SWIR1	12	74	1556.20	1556.70	14.80
SWIR1	13	75	1569.30	1569.80	14.50
SWIR1	14	76	1582.30	1582.80	14.70
SWIR1	15	77	1595.20	1595.70	14.90
SWIR1	16	78	1608.30	1608.80	14.50
SWIR1	17	79	1621.10	1621.60	14.40
SWIR1	18	80	1633.90	1634.40	14.70
SWIR1	19	81	1646.70	1647.20	14.60
SWIR1	20	82	1659.40	1659.90	14.30
SWIR1	21	83	1671.70	1672.20	14.10

SWIR1	22	84	1684.10	1684.60	14.40
SWIR1	23	85	1696.70	1697.20	14.40
SWIR1	24	86	1709.00	1709.50	13.90
SWIR1	25	87	1721.20	1721.70	13.70
SWIR1	26	88	1733.30	1733.80	14.00
SWIR1	27	89	1745.50	1746.00	14.00
SWIR1	28	90	1757.50	1758.00	13.50
SWIR1	29	91	1769.40	1769.90	13.60
SWIR1	30	92	1781.20	1781.70	13.60
SWIR1	31	93	1793.10	1793.60	13.50
SWIR1	32	94	1804.90	1805.40	13.10
SWIR2	1	95	1951.10	1953.20	21.00
SWIR2	2	96	1969.90	1972.00	20.90
SWIR2	3	97	1988.60	1990.70	20.90
SWIR2	4	98	2007.30	2009.40	21.20
SWIR2	5	99	2026.00	2028.10	21.10
SWIR2	6	100	2044.70	2046.80	21.30
SWIR2	7	101	2063.20	2065.30	21.00
SWIR2	8	102	2081.20	2083.30	20.20
SWIR2	9	103	2098.80	2100.90	20.10
SWIR2	10	104	2116.50	2118.60	20.10
SWIR2	11	105	2134.20	2136.30	20.30
SWIR2	12	106	2151.90	2154.00	20.50
SWIR2	13	107	2169.50	2171.60	19.90
SWIR2	14	108	2186.20	2188.30	19.00
SWIR2	15	109	2203.10	2205.20	20.40
SWIR2	16	110	2221.30	2223.40	19.50
SWIR2	17	111	2238.00	2240.10	19.70
SWIR2	18	112	2255.50	2257.60	20.40
SWIR2	19	113	2272.30	2274.40	19.80
SWIR2	20	114	2289.00	2291.10	19.50
SWIR2	21	115	2305.40	2307.50	19.20
SWIR2	22	116	2321.50	2323.60	19.20
SWIR2	23	117	2337.70	2339.80	19.40
SWIR2	24	118	2354.20	2356.30	19.60
SWIR2	25	119	2370.40	2372.50	19.40
SWIR2	26	120	2386.40	2388.50	19.00
SWIR2	27	121	2402.20	2404.30	18.60
SWIR2	28	122	2417.80	2419.90	18.50
SWIR2	29	123	2433.30	2435.40	18.60
SWIR2	30	124	2448.80	2450.90	18.90
SWIR2	31	125	2464.50	2466.60	18.60
SWIR2	32	126	2479.90	2482.00	18.30

Appendix 8: HyMap QuickLooks

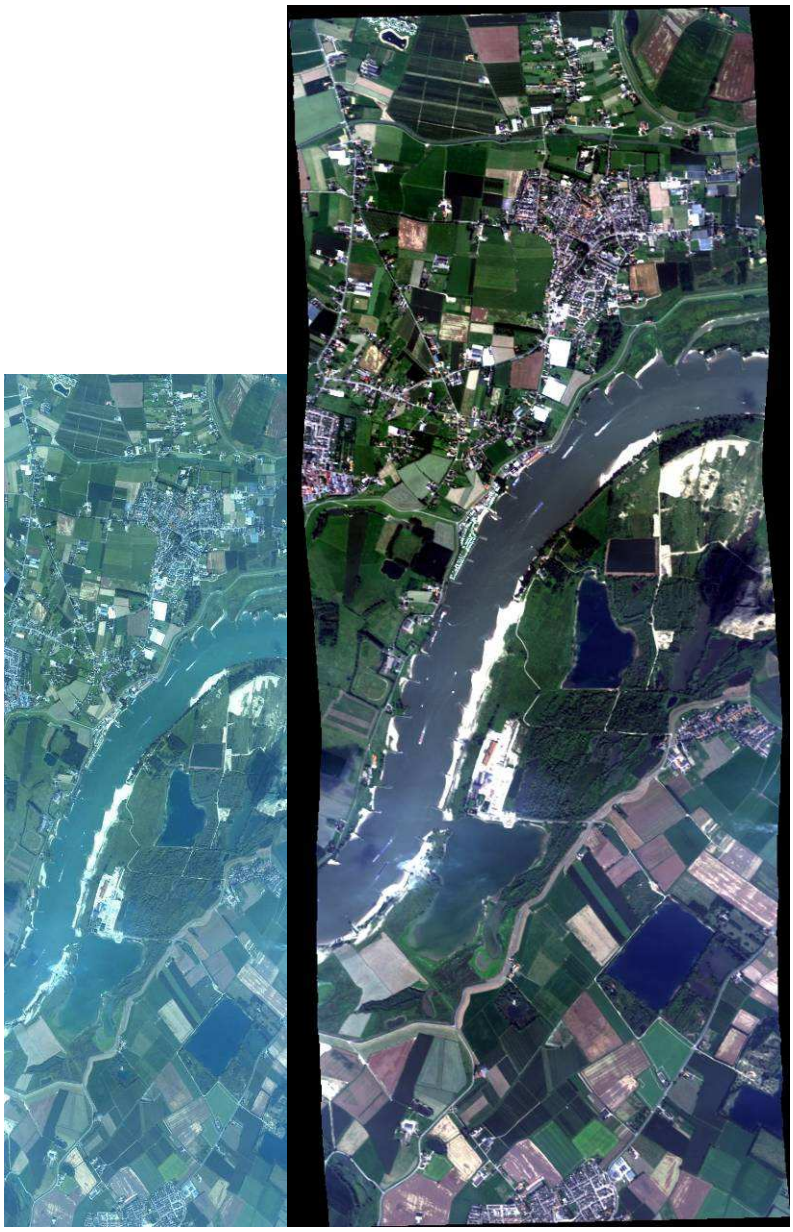

HyMap Quicklook ‘Millingerwaard’, 28. July 2004, Strip 1 (RGB = 15/10/5 (652.6 nm, 576.3 nm, 500.1 nm)) (left = Raw DLR quicklook, right = Geocoded and calibrated VITO quicklook).

Appedix 9: Critical values of the pearson product-moment correlation coefficient

df = *n* -2				
Level of Significance (p) for Two-Tailed Test	**.10**	**.05**	**.02**	**.01**
df				
1	.988	.997	.9995	.9999
2	.900	.950	.980	.990
3	.805	.878	.934	.959
4	.729	.811	.882	.917
5	.669	.754	.833	.874
6	.622	.707	.789	.834
7	.582	.666	.750	.798
8	.549	.632	.716	.765
9	.521	.602	.685	.735
10	.497	.576	.658	.708
11	.476	.553	.634	.684
12	.458	.532	.612	.661
13	.441	.514	.592	.641
14	.426	.497	.574	.623
15	.412	.482	.558	.606
16	.400	.468	.542	.590
17	.389	.456	.528	.575
18	.378	.444	.516	.561

19	.369	.433	.503	.549
20	.360	.423	.492	.537
21	.352	.413	.482	.526
22	.344	.404	.472	.515
23	.337	.396	.462	.505
24	.330	.388	.453	.496
25	.323	.381	.445	.487
26	.317	.374	.437	.479
27	.311	.367	.430	.471
28	.306	.361	.423	.463
29	.301	.355	.416	.456
30	.296	.349	.409	.449
35	.275	.325	.381	.418
40	.257	.304	.358	.393
45	.243	.288	.338	.372
50	.231	.273	.322	.354
60	.211	.250	.295	.325
70	.195	.232	.274	.303
80	.183	.217	.256	.283
90	.173	.205	.242	.267
100	.164	.195	.230	.254

http://www.gifted.uconn.edu/siegle/research/Correlation/corrchrt.htm

Appendix 10: Difference between two dependent correlations, thus, from a single sample.

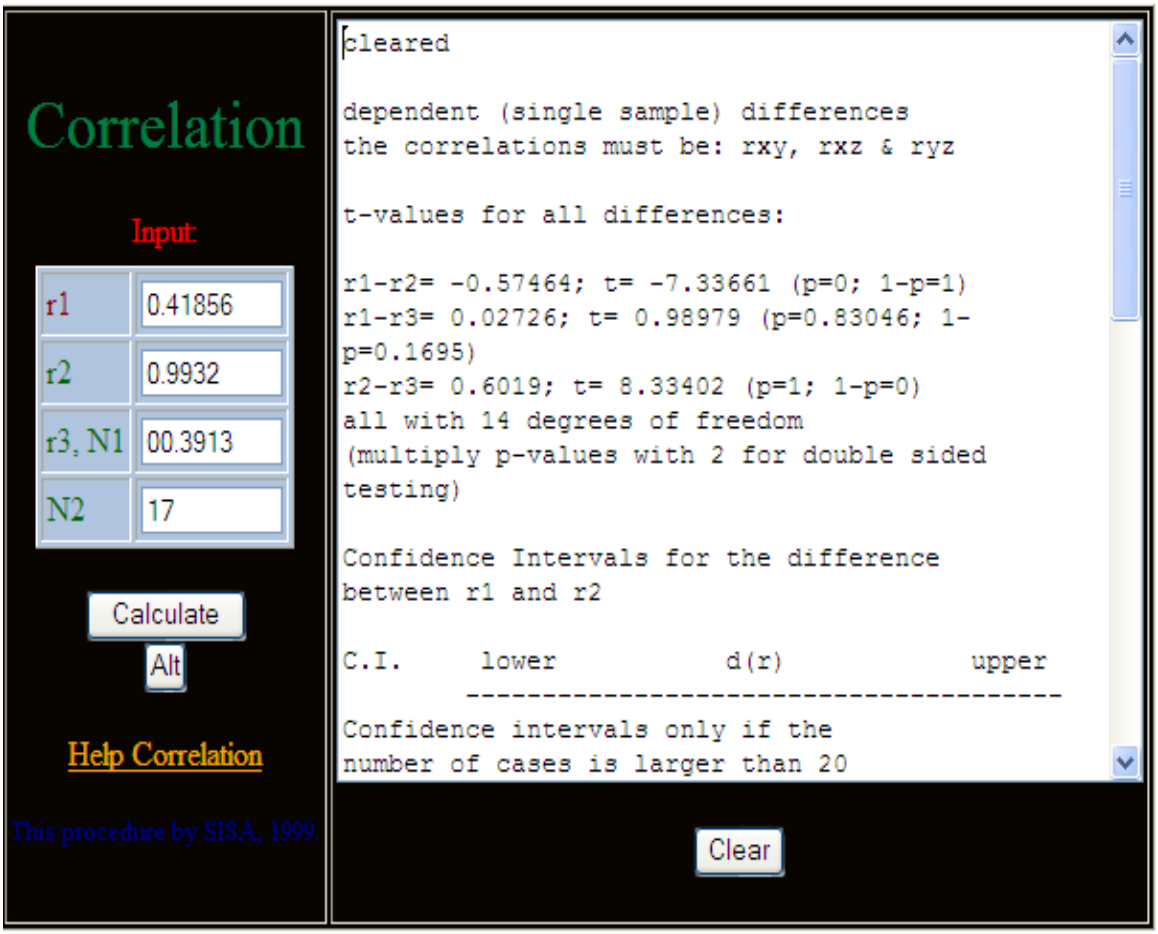

Example 1: checking the effect of MBD and AUC on estimation of DW at water absorption feature 970 nm in HyMap image considering only one pixel for each sample plot.

dependent (single sample) differences
the correlations must be: rxy, rxz & ryz

t-values for all differences:
r1-r2= -0.57464; t= -7.33661 (p=0; 1-p=1)
r1-r3= 0.02726; t= 0.98979 (p=0.83046; 1-p=0.1695)
r2-r3= 0.6019; t= 8.33402 (p=1; 1-p=0)
all with 14 degrees of freedom
(multiply p-values with 2 for double sided testing)

Confidence Intervals for the difference
between r1 and r2

C.I.	lower	d(r)	upper

Confidence intervals only if the
number of cases is larger than 20
R1 is the correlation between Y and X
R2 is the correlation between Y and Z
R3 is the correlation between X and Z

correlation between Y and X
Simple (r(yx)): 0.41856 Partial (r(yx.z)): 0.2793
correlation between Y and Z
Simple (r(yz)): 0.9932 Partial (r(yz.x)): 0.9924
correlation between X and Z
Simple (r(xz)): 0.3913 Partial (r(xz.y)): -0.2309

ANOVA table (variance explained in Y by x & z):

	Total in Y	= expl. + added = by X	+ by Z* by X	* not expl.
R-sq:	|0.9875	=0.1752	+0.9848	*0.8248
F:	|553.2	|3	|910	
df:	|7	|14	|14	
p-val:	|0	|0.1066	|0	

more

Confidence Intervals for R (Y.xz)
(Optimistic C.I. for correlation for Y on x&z)

C.I.	lower		Ry.xz		upper
80%	0.986906	<	0.9937	<	0.997005
90%	0.983877	<	0.9937	<	0.997571
95%	0.980692	<	0.9937	<	0.997974
99%	0.972575	<	0.9937	<	0.998579

Example 2: checking the effect of MBD and MBD/AUC on estimation of DW at water absorption feature 970 nm in HyMap image considering only one pixel for each sample plot.

Dependent (single sample) differences
the correlations must be: rxy, rxz & ryz

t-values for all differences:
r1-r2= 0.44996; t= 1.12058 (p=0.85934; 1-p=0.1407)
r1-r3= 0.73846; t= 2.2489 (p=0.97943; 1-p=0.0206)
r2-r3= 0.2885; t= 1.06219 (p=0.84693; 1-p=0.1531)
all with 14 degrees of freedom
(multiply p-values with 2 for double sided testing)

Confidence Intervals for the difference
between r1 and r2
C.I. lower d(r) upper

Confidence intervals only if the
number of cases is larger than 20
R1 is the correlation between Y and X
R2 is the correlation between Y and Z
R3 is the correlation between X and Z

correlation between Y and X
Simple (r(yx)): 0.41856 Partial (r(yx.z)): 0.4314
correlation between Y and Z
Simple (r(yz)): -0.0314 Partial (r(yz.x)): 0.1191
correlation between X and Z
Simple (r(xz)): -0.3199 Partial (r(xz.y)): -0.3379

ANOVA table (variance explained in Y by x & z):

	Total in Y	= expl. + added = by X	+ by Z* by X	* not expl.
R-sq:	|0.1869	=0.1752	+0.0142	*0.8248
F:	|1.6	|3	|0.2	
df:	|7	|14	|14	
p-val:	|0.2661	|0.1066	|0.6604	

more

Confidence Intervals for R (Y.xz)
(Optimistic C.I. for correlation for Y on x&z)

C.I.	lower		Ry.xz		upper
80%	0.092394	<	0.4323	<	0.681988
90%	-0.01213	<	0.4323	<	0.734122
95%	-0.1027	<	0.4323	<	0.773323
99%	-0.273459	<	0.4323	<	0.835499

http://www.quantitativeskills.com/sisa/statistics/correl.htm